Population dispersal via diffusion-reaction equations

Anne Kandler[1]
University College London, London,UK

Roman Unger
Technical University Chemnitz, Chemnitz, Germany

Abstract. Diffusion-reaction systems are well-established in different life-science disciplines. When applied to 'human questions' they are used to estimate the demographic processes involved in major human (or animal) dispersal episodes and to estimate the general spread pattern of new ideas or technologies through cultures. This manuscript gives an introduction to diffusion-reaction systems for a non-mathematical audience. We focus on describing dispersal processes and start with modelling and analysing the spread dynamic of a single population under different dispersal and growth hypotheses. Further, we focus on the impacts of population interactions on spread behaviour of a particular population. Lastly we introduce an open software package 'CultDiff' which provides a solution tool for diffusion reaction systems.

Keywords. Population dispersal, population growth, diffusion-reaction system, random walk, Lotka-Volterra system, 'CultDiff'.

---

[1] Correspondence concerning this manuscript should be addressed to Anne Kandler, Institute of Archaeology, University College London, 31-34 Gordon Square, London WC1H 0PY, UK (email: a.kandler@ucl.ac.uk)

Contents

1 Introduction

Diffusion-reaction systems have proven to be a powerful tool for describing spatial dispersal processes. R.A. Fisher developed in 1937 the now classic Fisher model[2] for the spread of an advantageous mutation ([17]). Using a diffusion model that incorporated the joint effect of selection and dispersal, Fisher showed that, after a gene was established in a population there would be a wave of advance for which the velocity of the wave is proportional to the selective advantage of the allele.

J.G. Skellam ([49]) used, in his pioneering paper 'Random dispersal in theoretical populations', a similar framework for theoretical studies of population dispersal and introduced the diffusion-reaction equation to ecology. He established the relationship between random walks as a description of movement of individual members of biological species and the diffusion equation as a description of dispersal of the population as a whole ([9]). Skellam was particularly interested in diffusion-reaction models for the population density of species in a bounded habitat assuming Malthusian and logistic population growth models. Among various other examples he presented in [49] a case study of the spread of the muskrats in Central Europe which became one of the standard examples for a wave-of-advance dispersal pattern. In 1905 several muskrats escaped into freedom near the Moldau river. Radial dispersal and exponential growth was recorded afterwards[3] (cf. Figure 1 for the location of the dispersal front for the time period 1905-1927). It turned out that Skellam's wave-of-advance model predictions fitted the actual data very well.

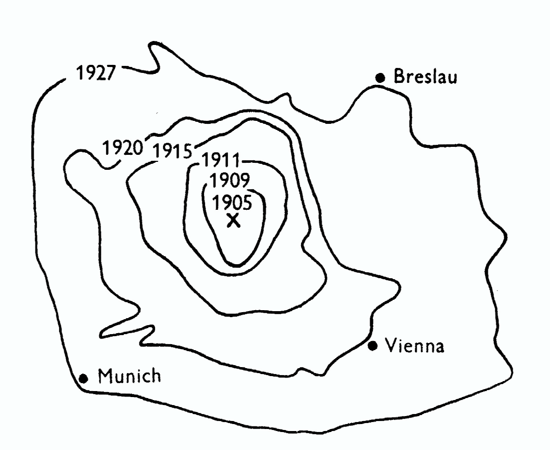

Figure 1: Spread of muskrats in Central Europe, 1905-1927, from [49]

Subsequently this modelling framework has been applied to human dispersal and the spread of innovations. One of the earliest studies was undertaken by Ammerman and Cavalli-Sforza ([2],[3]) who analysed the spread of early farming in Europe. Agriculture spread into geographical areas previously occupied by hunter-gatherers around 10,000

---

[2] Often the model is called Fisher-Kolmogorov-Petrovski-Piskunov model to acknowledge the contribution of the mathematicians A. Kolmogrov, I.Petrovski and N. Piskunov in developing the mathematical theory of diffusion-reaction equation.(cf. [29])

[3] Although the muskrat has many natural predators, in this case there was no nature-imposed carrying capacity during the first years.

years ago. Ammerman and Cavalli-Sforza ([2]) applied a diffusion-reaction model to interpret archaeological dating of the arrival of agriculture in various European locations. They estimated that the spread of farming to Europe from the Middle East occurred at a rate of about 1 kilometer per year which proves to be consistent with the spreading speed predicted by the diffusion-reaction model with ethnographically derived values for the model parameters. By studying geographical variation in gene frequencies over the same area, Ammerman and Cavalli-Sforza ([3]) suggested that this spread was due to physical migration of the farmers rather than to the spread of the cultural idea of farming. More recent extensions of this analysis have involved more detailed models of demography and rates of cultural conversion of hunter-gatherers to farmers ([4]), but the results are qualitatively similar.

Young and Bettinger [55] and Steele and colleagues (e.g. [22],[51]) applied the diffusion-reaction approach to Palaeolithic dispersal. Steele et al. considered in [51] hunter-gatherer dispersal into North America south of the ice sheets using diffusion-reaction models. Under simplified assumptions they modelled the archaeological signature of a dispersal process using archaeological data (time-averaged artefact and site densities) as indicators. They showed that where this dispersal process involved movement up gradients of carrying capacity (as in dispersal towards the southeast from a possible origin in Alberta), the cumulated density of evidence for human occupation would be greatest in the more productive environments and the initial pioneer gradient washed out when the indicator artefact maps have been time-averaged over one thousand years or more (cf. Figure 2).

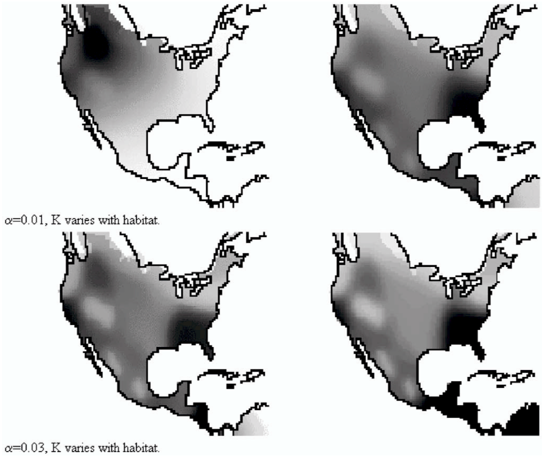

Figure 2: Cumulative occupancy of North America by a colonizing population over the first 1000 years (left-hand maps) and over the first 2000 years (right-hand maps). From [51].

Recent studies aim to determine the speed of the spread of anatomically modern human into Europe before the last glacial maximum ([35]), the rate of subsequent late glacial recolonisation of Northern Europe as the ice receded ([26],[18]) or the diffusion of Clovis spear point technology in late glacial North America ([21]). A comprehensive overview regarding diffusion-reaction models applied to human dispersal can be found in [50].

Further, diffusion-reaction equations have been applied to the field of diffusion of innovations. Generally, the theory of diffusion of innovations is concerned with the how, why and at what rate new ideas and technologies spread through a population ([48]). Henrich's study ([23]) focuses on especially the early phase of the adoption of the hybrid corn in U.S. using a social learning model which resembled a modified logistic growth model. This model was generalised in [27] by adding a diffusion component and therefore adding a spatial dimension to the model.

We can conclude that diffusion-reaction equations are now established in different life-science disciplines and when applied to 'human questions' are used to estimate the demographic process involved in major human (or animal) dispersal episodes ([50]) or the general spread pattern of new ideas or technologies through cultures. Our aim in the following is to give an introduction into the fundamentals of this modelling approach without getting lost in technical details. So when writing this paper we had a non-mathematical audience in mind and therefore lengthy algebraic exercises are left out wherever possible. Nonetheless we have included sections marked with ($\star$) and 'grey boxes' on places in the text were the mathematically interested reader might want to know a bit more about the "how it is done mathematically". However, for the general understanding of the paper these sections and boxes are not necessary.

We start in section 2 by studying the fundamental features of random walks and derive, based on the random walk theory, the general diffusion equation. Section 3 focuses on the modelling of growth processes. We introduce four growth models (exponential growth, logistic growth, confined exponential growth, Gompertz growth) and analyse the resulting growth dynamic. Further, we discuss the applicability of these models to different real-world situations. In section 4 we combine both, the dispersal and the growth components and derive the main characteristics of the obtained diffusion-reaction models. In section 5 we focus on the impacts of population interactions on the spread behaviour of a particular population. There we consider prey-predator and competition situations. In the last part we introduce the open software package 'CultDiff' which provides a solution tool for diffusion-reaction systems.

The structure of the paper and many considerations are influenced by the wonderful textbooks by [7],[41],[44] and [9].

The authors would like to acknowledge Dr. James Steele for helpful and encouraging discussions during the development of 'CultDiff' and the process of writing this manuscript. Further, we thank Charlotte Frearson for careful proofreading of the manuscript.

2 Diffusion

The concept of diffusion originates from physical sciences (Fick's law is regarded as the fundamental principle of diffusion, cf. box 1 for a more detailed consideration). In its physical sense diffusion is defined as a phenomenon where a certain particle group as a whole spreads according to the irregular motion of each particle. Thereby the spread is always directed from regions of higher concentration to regions of lower concentration and the time dependence of the distribution of the particles in space is given by the so called diffusion equation which is the mathematical formulation of the described spread dynamic. The diffusion theory seeks to explain the spread behaviour of a group of particles (rather than spread behaviour of a single particle) and consequently the variable of interest is the proportion of the particle group which can be found in location x at time t. In this way phenomena like the diffusion of an ink drop in water[4] or diffusion of heat can be described.

Excursus into the physical theory. The classical theory of diffusion was founded in 1855 by the physiologist Adolf Fick ([16]). Fick's law postulates that the transport of matter, i.e. the flux, goes from regions of high concentration to regions of low concentration, with a magnitude that is proportional to the concentration gradient of the matter. It yields

$$\frac{\partial C}{\partial t} = -\frac{J_x}{\partial x} = \frac{\partial}{\partial x}\left(D\frac{\partial C}{\partial x}\right) \tag{1}$$

where the variable C describes the concentration of the matter at time t and location x, $\frac{\partial C}{\partial t}$ models the temporal change of the concentration, J_x the flux of C in x direction across a unit normal area in a time unit and D stands for the diffusivity. If D is constant equation (1) has the explicit solution (under the assumption that initially M particles in a unit area are concentrated at $x = 0$)

$$C(t,x) = \frac{M}{2\sqrt{\pi D t}} exp\left(-\frac{x^2}{4Dt}\right) \tag{2}$$

([7]). If we compare equation (3) with the just derived solution (2) we see that Fickian diffusion is only applicable to phenomena that are based on the random walk hypothesis of the particle.

Applications of the diffusion theory outside physics were pioneered by the French mathematician Louis Bachelier who used a random walk model to describe price fluctuations on financial markets ([6]). Amongst others the concept of diffusion is applied in biology to describe processes of biodiffusion and to model population dynamics, or in a less quantitative way, in social sciences to describe the spread of ideas (diffusion of innovations, lexical diffusion, trans-cultural diffusion).

In the following we understand diffusion as the dispersal mechanism of populations and derive the model's merits but also its limitations when applied to situations of human dispersal. However, we stress that the theory is equally applicable to problems of the spread of new ideas or technologies through spatially structured populations.

A crucial element of the diffusion theory is the assumption of the 'irregular' motion performed by each individual. Every individual is expected to move in random patterns which we will specify as a random walk. However, the diffusion theory describes the spread of a population on the population level by determining the frequency of individuals of the dispersing population at every time t and location x. In order to understand the implication of the assumed random walk hypothesis on the population dispersal pattern we derive the fundamental diffusion equation from this random walk assumption.

---

[4] This short video clip (http://www.youtube.com/watch?v=H7QsDs8ZRMI&feature=related) illustrates the physical phenomenon of diffusion nicely.

2.1 The random walk

As the name suggests random walks are based on the intuitive idea of taking successive steps (of random or deterministic length), each in a random direction. Mathematically a random walk is classified as a stochastic process[5]. We start with analysing the one-dimensional random walk, a random walk along a line, and generalise the obtained results in section 2.1.2 for the two-dimensional case.

Some historical remarks. The botanist Robert Brown is traditionally regarded with the discovery of continuous 'jittery' motion which was later called 'Brownian motion' in 1827. It is believed that Brown was studying pollen particles floating in water under the microscope. He then observed minute particles within the vacuoles of the pollen grains executing a jittery motion. By repeating the experiment with particles of dust, he was able to rule out that the motion was due to pollen particles being 'alive'. However, Brown did not provide a theory to explain the motion.
The first person to describe the mathematics behind Brownian motion was Thorvald N. Thiele in 1880 in a paper on the method of least squares. This was followed independently by Louis Bachelier in 1900 in his PhD thesis 'Théorie de la spéculation', in which he presented a stochastic analysis of the stock and option markets. However, it was Albert Einstein ([14]) and Marian Smoluchowski ([53]) who independently brought the solution of the problem to the attention of physicists, and presented it as a way to indirectly confirm the existence of atoms and molecules.

2.1.1 1-Dimensional random walk

We assume an integer number line $\mathbb{Z}$ where the numbers are spaced apart equally (cf. Figure 3).

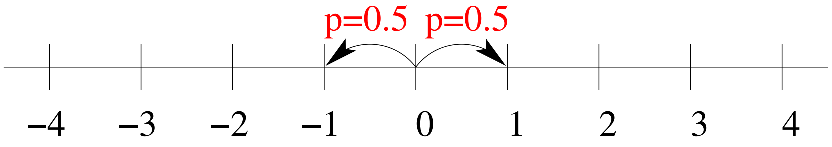

Figure 3: Schematic illustration of a symmetric random walk along the number line

An elementary and concrete random walk starts at $S_0 = 0$ and at each step moves one unit either to the left or the right with equal probability. To define this walk formally, we introduce independent random variables $Z_1, Z_2, \ldots$. Each variable Z_i identifies either a move to the left or to the right (that means $Z_i = -1$ for a move to the left and $Z_i = 1$ for a move to the right) with a 50% probability for either value. Now we set

$$S_n := \sum_{j=1}^{n} Z_j.$$

---

[5] A stochastic process describes the evolution of a random variable over time and space.

The series $\{S_n\}$ (the sum of the sequence of -1's and 1's) describes a simple random walk on $\mathbb{Z}$ and characterises the position of the random walk after n time steps (if each part of the walk has length one). In order to simulate such an one-dimensional symmetric[6] random walk we simply follow the three steps listed below.

1. Place an individual at $x = 0$ on the line.
2. It moves with probability 0.5 one step either to the right or to the left.
    - Flip a coin.
    - If you get a head, move one step right, else move one step left.
3. Repeat step (2) a total of n times.

So, if we flip the coin 5 times and get HTHHH, then the movement will be:

$$0 \rightarrow 1 \rightarrow 0 \rightarrow 1 \rightarrow 2 \rightarrow 3,$$

and we end up at 3. Of course, the "reverse" sequence is possible: THTTT, and you end up at -3. In fact, the only positions you can end up at with 5 tosses are 1, -1, 3, -3 ,5, and -5. However, there are different probabilities for reaching these positions (cf. Figure 4):

- for position 1 (means 3 heads and 2 tails) 10 sequences are possible
- for position -1 (means 2 heads and 3 tails) 10 sequences are possible
- for position 3 (means 4 heads and 1 tail) 5 sequences are possible
- for position -3 (means 1 head and 4 tails) 5 sequences are possible
- for position 5 (means 5 heads) only 1 sequence is possible
- for position -5 (means 5 tails) only 1 sequence is possible

Due to the assumed symmetry of the random walk there are as many ways to be at 1 as there are to be a -1; similarly for 3 and -3 and 5 and -5.

The position S_n of the random walk after n steps is random and therefore cannot be predicted. However, we can say that in the long run, the most likely position of the random walk would be at 0. In other words the expected value, $\mathbb{E}S_n$, of the random walk is 0. Generally, to calculate the expected value of a stochastic process, multiply each possible outcome of the process by its probability, and add up the results. In our case we have

$$\mathbb{E}S_5 = \sum_{i=1}^{5} x_i p(x_i) = 1 * \frac{10}{32} + (-1) * \frac{10}{32} + 3 * \frac{5}{32} + (-3) * \frac{5}{32} + 5 * \frac{1}{32} + (-5) * \frac{1}{32} = 0$$

---

[6] To generate an asymmetric random walk you need to choose the probabilities of moving to the right or left not equally.

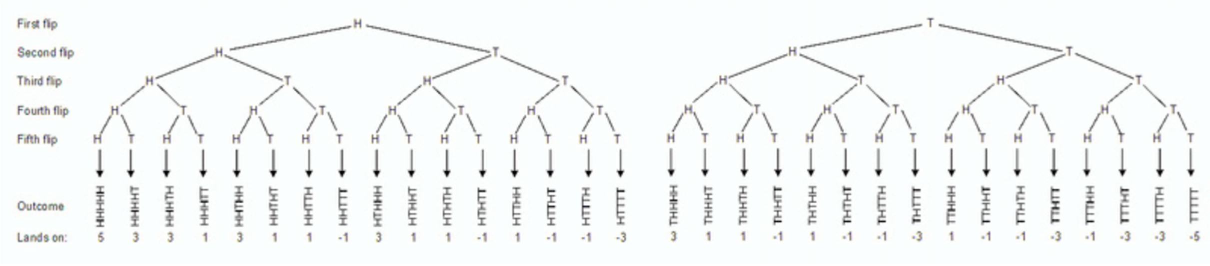

Figure 4: Possible outcomes for a sequence of five coin flips.

where x_i stands for the possible outcomes -5,-3,-1,1,3,5 and $p(x_i)$ for their probability. There are 32 possible outcomes to a series of five subsequent coin tosses and therefore the probability of being e.g. at 1 is 10/32.

We are not only interested in the expected position of the random walker but also in how far the random walker has moved. So after five coin flips, what is the expected distance from the origin 0? The ansatz for this computation in general is to find not the expected value of the distance, but the expected value of the squared distance[7].

$$\begin{aligned}\mathbb{E}(S_5)^2 &= \sum_{i=1}^{5} x_i^2 p(x_i) \\ &= 1^2 * \frac{10}{32} + (-1)^2 * \frac{10}{32} + 3^2 * \frac{5}{32} + (-3)^2 * \frac{5}{32} + 5^2 * \frac{1}{32} + (-5)^2 * \frac{1}{32} = 5.\end{aligned}$$

The expected mean squared distance is 5, hence the expected root mean squared distance from the origin after 5 coin flips is $\sqrt{5}$ and we can derive a very general theorem.

Theorem 1. The expected root-mean square distance from the origin after n steps of a symmetric random walk with step length one is $\sqrt{n}$.

Figure 5 (left) shows several realisations of one-dimensional random walks. We clearly see the random nature of the movements but also the increasing distance from the origin 0 as time progresses (what confirms theorem 1).

Remark 1. A random walk having a step size that varies according to a normal distribution is used as a model for real-world time series data such as financial markets. The Black-Scholes formula for modeling equity option prices, for example, uses a Gaussian random walk as an underlying assumption.

Theorem 2. For step length distributed according to any distribution with a finite variance σ^2 (not necessarily just a normal distribution), the root mean squared expected distance after n steps is $\sigma\sqrt{n}$.

---

[7] The calculation of the variance follows the same principle.

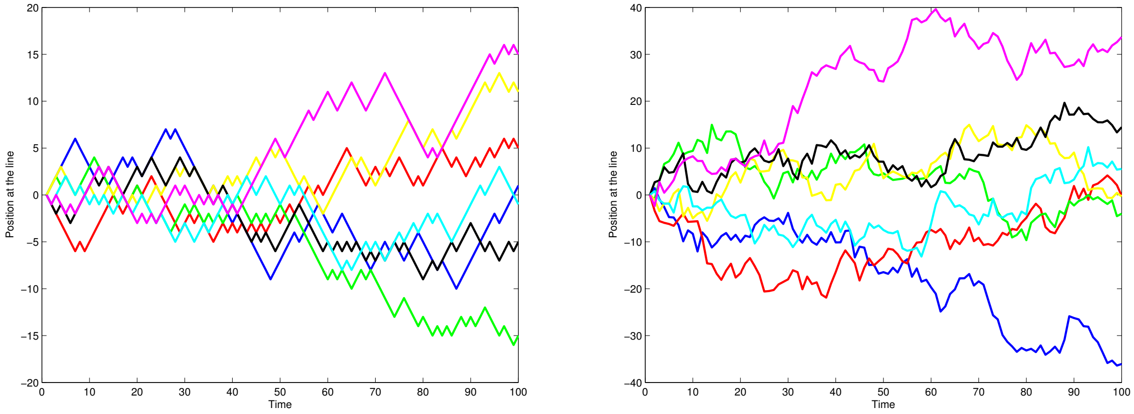

Figure 5: Seven realisations of a symmetric random walk with step length 1 (left Figure) and normally distributed (with the parameter $\mu = 0$ and $\sigma^2 = 4$) step length (right Figure).

2.1.2 2-Dimensional random walk

The two-dimensional random walk on a lattice is a straightforward generalisation of the one-dimensional random walk. Instead of only moving to the left or to the right we allow the random walker to move to one of the four neighbouring lattice points with probability 0.25 (cf. Figure 6).

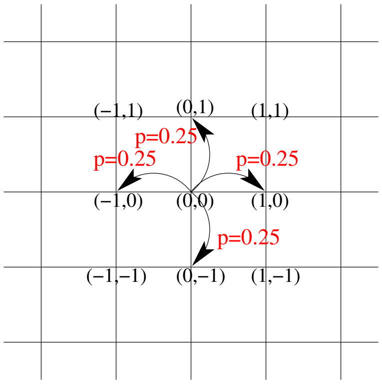

Figure 6: Schematic illustration of a symmetric random walk along the lattice

In order to simulate a two-dimensional symmetric random walk on a lattice we simply perform the following 4 steps

1. Start at the origin (0,0).
2. Choose a direction randomly from the set $\{1, 2, 3, 4\}$ where 1 means step to the left, 2 to the right, 3 to the bottom and 4 to the top (cf. Figure 6)
3. Take one step in the chosen direction.
4. Repeat steps (2) and (3) a total of n times.

Figure 7 (left) shows realisations of such a random walk. It can be proven that on a two-dimensional lattice, a random walk has probability 1 of reaching any point (including the starting point) as the number of steps approaches infinity.

More generally, two-dimensional random walks do not need to follow the lattice structure. Steps 2. and 3. in the simulation procedure can be replaced by:

2. Choose an angle randomly from 0 to 360 degrees (0 to 2*pi radians)[8].
3. Take one step in the direction of the angle (measured from the horizontal direction).

Figure 7 shows realisations for both two-dimensional random walk constructions. Again we observe the random nature of the spread process.

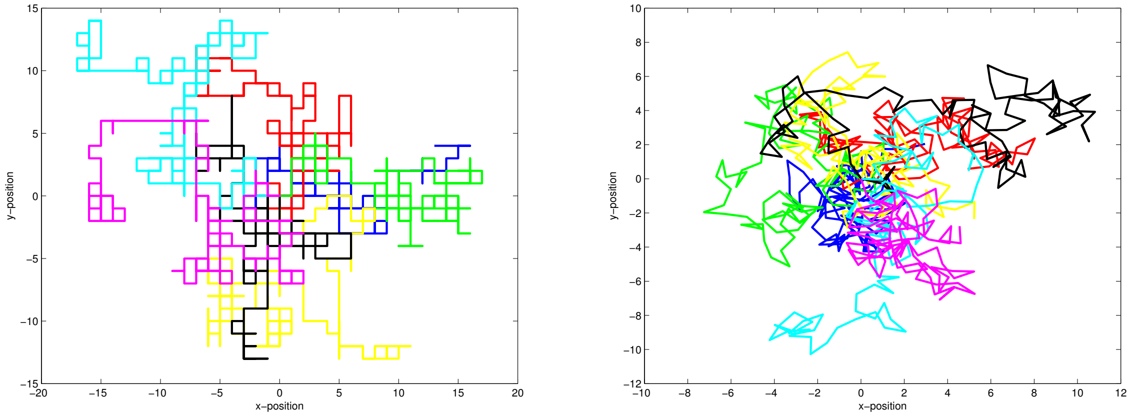

Figure 7: Seven realisations of a symmetric random walk with step length 1 on the lattice (left figure) and with randomly chosen directions (right figure).

It turns out that the theorem 1 is true for 2-dimensional random walks. So, the expected root-mean square distance from the origin (0,0) after n steps of a symmetric two-dimensional random walk with step length one is $\sqrt{n}$.

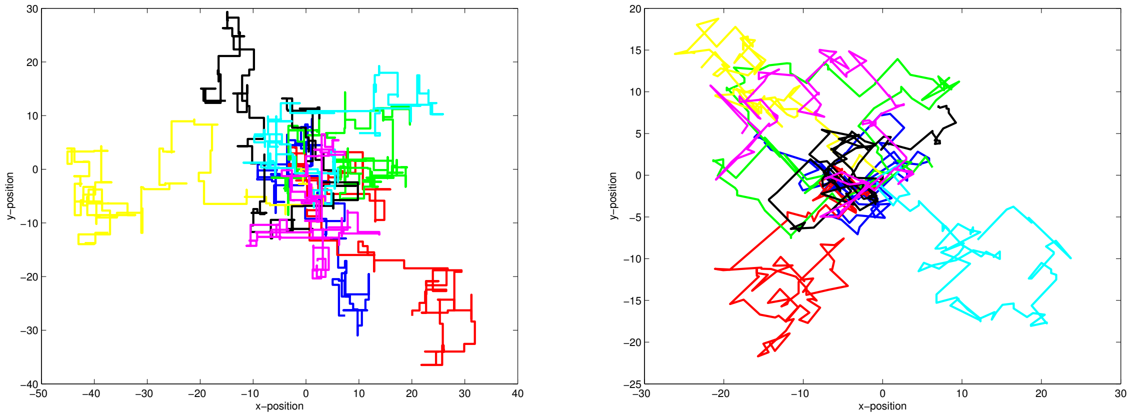

Figure 8: Seven realisations of a symmetric random walk with normal distributed step length (with the parameter $\mu = 0$ and $\sigma^2 = 4$) on the lattice (left Figure) and with randomly chosen directions (right Figure).

---

[8] In order to choose the angle randomly we need a random number generator.

Analogous to Remark 1 we can generalise the two-dimensional random walk to a Gaussian two-dimensional random walk by assuming normal distributed step lengths. Figure 8 shows realisation of those Gaussian random walks on a lattice (left Figure) and with randomly chosen direction (right Figure).

2.1.3 Applications

Random walks have been applied to numerous and also very different fields of research.

- Traditionally random walks are used in physics as simplified models of Brownian motion and the random movement of molecules in liquids and gases.
- Applied to mathematical ecology, random walks are used to describe individual (animal or even human) movements to model processes of biodiffusion and population dynamics.
- In the finance sector, the random walk model is used to describe the fluctuating movements of stock prices and other financial factors (However, empirical studies found evidence for deviations from this theoretical model, especially due to the existence of short and long term correlations).
- In population genetics the random walk hypothesis is used to analyse genetic drift.
- Probability models in lotteries and Las Vegas casinos use random walk models in slot machines and to catch cheaters
- Google uses a random walk model in its search engine to provide the most relevant search results
- The steel sections of Antony Gormley's Quantum Cloud were arranged using a computer model with a random walk algorithm starting from points on the surface of an enlarged figure based on Gormley's body that forms a residual outline at the centre of the sculpture.

Figure 9: Antony Gormley's Quantum Cloud

- During World War II a random walk was used to model the distance that an escaped prisoner of war would travel in a given time.

2.2 Diffusion model

Based on our gained insights from the theory of random walk we now develop the general diffusion theory. We are especially interested in deriving spatial distribution results of the dispersing population. In other words we assume a population with a sufficient high number of individuals situated at $x = 0$ at time $t = 0$ and are interested in the spatial distribution of this population as time progresses. That means we determine the proportion of the population at any location x and time t under the assumption that all individuals perform a random walk. This proportion is expressed by the continuous variable $u(t, x)$. Here we carry out the transition from discrete considerations in time and space to continuous considerations in time and space[9].

Figure 11 shows temporal change of the population distribution under the assumption that every individual performs a random walk along a line.

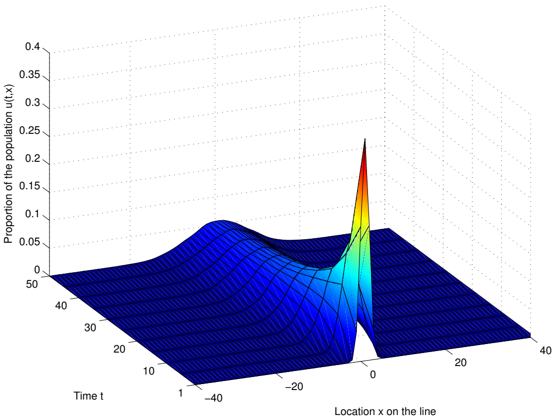

Figure 10: Spatial distribution of the population initially located at $x = 0$ for different times t. This Figure shows the relative population density, so $u(t, x) \in [0, 1]$.

Two effects are immediately obvious.

- With progressing time the population is averaged out over space. We observe a dispersal behaviour which is directed from highly populated areas to less populated areas and the system reaches its equilibrium[10] if there are the same number of individuals in every location x.
- The frequency distributions at times t of the population consisting of M individuals

---

[9] This fact implies that the diffusion approach is only suited for large populations.

[10] Equilibrium means in this case that the proportion of the population u does not change over time any more.

follows a normal distribution. It yields

$$u(x,t) = \frac{M}{2\sqrt{\pi D t}} exp\left(-\frac{x^2}{4Dt}\right) \tag{3}$$

which is the solution of the diffusion equation

$$\frac{\partial u}{\partial t}(t,x) = D\triangle u(t,x). \tag{4}$$

The mathematical symbol $\triangle$ defines the Laplacian operator, which is the mathematical description of the process of moving the population from local spatial regions of high density to those of a lower density and D is the diffusivity affecting the rate at which the population moves down these gradients. The higher D the faster the dispersal occurs.

Mathematical derivation of the diffusion equation. We derive the recursion equation for the probability $p(t,x)$ that a single particle is at time t at point x or equivalently the fraction of a population of individuals that are at location x at time t. This equivalence is given due to the independence of the individual motions in this simple model. Given the spatial and temporal step lengths Δx and Δt the recursion equation on p takes the form

$$p(t,x) = \frac{1}{2}p(t-\Delta t, x+\Delta x) + \frac{1}{2}p(t-\Delta t, x-\Delta x)$$

because of the assumption that all individuals move every time step. Expanding the right hand side into a Taylor series we obtain

$$\frac{\partial p}{\partial t} = \left(\frac{(\Delta x)^2}{2\Delta t}\right)\frac{\partial^2 p}{\partial x^2} + \left(\frac{\Delta t}{2}\right)\frac{\partial^2 p}{\partial t^2} + \dots$$

To derive a continuous approximation of this formulation Δx and Δt must tend to zero in a manner that the limit

$$D = \lim_{\lambda,\tau\to 0}\frac{\lambda^2}{2\tau}$$

exists. We obtain

$$\frac{\partial p}{\partial t} = D\frac{\partial^2 p}{\partial x^2}.$$

If the total number of released particles is M then the concentration of particles is given by $u(t,x) = Mp(t,x)$.

Summarising we can say, that the diffusion model is built on the random walk hypothesis for the individual's movement, however, its strength lies in the macro-level description of the populations dispersal pattern in time and space. Equation (4) establishes the relationship between random walks as a description of movement of individual members of some theoretical biological species and the diffusion equation as a description of dispersal of the population as a whole ([9]). We have seen that the dispersal is always directed from regions of high population density to regions of low density and the speed of this dispersal is determined by the diffusivity D.

2.2.1 Applications

The diffusion equation arises in the modeling of a number of different phenomena.

- The classical application in physics of equation (4) is to model heat transfer. Often the diffusion equation is also called the heat equation.
- The diffusion equation is often used in financial mathematics to model the behaviour of options. The famous Black – Scholes option pricing formula can be transformed into the diffusion equation.
- The diffusion equation is also used to describe the spread of pollutants in water and air.

2.3 Criticisms of the diffusion model*

The main criticism of the diffusion model can be summarised by the model's implication that individuals proceed with infinite velocity along completely random paths ([25]). However, these in the literature often cited objections sound misleadingly drastic. The infinite velocity is caused by a positive, although infinitesimally small, probability of an individual moving an infinite distance from its present position. The complete random paths are caused by deriving the spatial dispersal behaviour of the population based on the assumption that each individual performs a symmetric random walk. This means the individual's movement becomes unpredictable even on the shortest scale ([25]). In section 2.3.1 we address these problems by replacing the random walk hypothesis with a correlated random walk model.

Further, we have seen that the resulting spatial distribution of the dispersal of a diffusive population is normal (cf. equation (3)). But this hypothesis is partly disproved by empirical consideration. There are a number of examples where the dispersal distribution shows no normal but rather a leptokurtic pattern.

In the following we briefly introduce two generalisations of the diffusion theory which address the listed problems.

2.3.1 Correlated random walk

Various statistical analysis, especially for the movements of animals, have shown that their motions during a certain period of time have a tendency to proceed in the same direction as in the period before (e.g. [44]). This leads to successive movements which are not mutually independent. The random walk model, however, includes the assumption that all successive movements are independent. Goldstein [20] proposed a random walk model with correlated steps. The idea is that individuals are more likely to proceed in the direction of the previous movement. The correlation coefficient γ, a measure for the strength of this 'following' tendency between successive steps, is introduced.

If we now replace in the derivation of the diffusion equation the random walk hypothesis by a random walk with correlated steps then the result is a slightly different equation, the so called telegraph equation. The telegraph equation possesses elements from the diffusion and wave motion and has properties which seem to be more realistic than those of the diffusion equation to describe animal motion (cp. [44]). In particular, the dispersal velocity is finite and the random paths become predictable on shorter scales.

Mathematical derivation of the telegraph equation. The derivation of the telegraph equation from a discrete correlated random walk is analogous to the derivation of the diffusion equation from a random walk (see [44],[25] for details). We obtain

$$\frac{\partial p}{\partial t} = -\frac{T}{2}\frac{\partial^2 p}{\partial t^2} + \frac{v^2 T}{2}\frac{\partial^2 p}{\partial x^2} \tag{5}$$

where v is the individuals finite velocity and T is the duration of the walk correlation. The telegraph equation possesses both diffusion and wave motions. However for $t >> T$ the telegraph equation (5) can be approximated by a diffusion equation of the form

$$\frac{\partial p}{\partial t} = \frac{v^2 T}{2}\frac{\partial^2 p}{\partial x^2}$$

where the diffusivity is expressed by $v^2T/2$ [44].

However, if we are interested in time periods which are much longer than the duration of the walk correlation the differences between the solutions of the diffusion and telegraph equation (that means the obtained population dispersal under the random walk and the correlated random walk hypothesis, respectively) are negligible (see Figure 11 and [25] for a discussion).

2.3.2 Leptokurtic distribution of dispersal

The diffusion model (4) predicts that the dispersal pattern of the population can be described by a normal distribution. However, this hypothesis is challenged by empirical results. Drobzhansky and Wright found that the spatial dispersal distribution of Drosophila does not show a normal but rather a leptokurtic shape ([12]). In terms of shape, a leptokurtic distribution has a more acute peak around the mean (meaning a higher probability than a normally distributed variable of values near the mean) and fatter tails (meaning a higher probability than a normally distributed variable of extreme values) (cf. Figure 12 where the blue lines represents a normal distribution and the red and green lines two leptokurtic distributions). This finding has been confirmed by a number of statistical analyses for different dispersal patterns (e.g. dispersal of ringed birds in England and Ireland [46], dispersal of freshwater killifish [19]). Interestingly, data on human dispersal also challenges the normal distribution assumption.

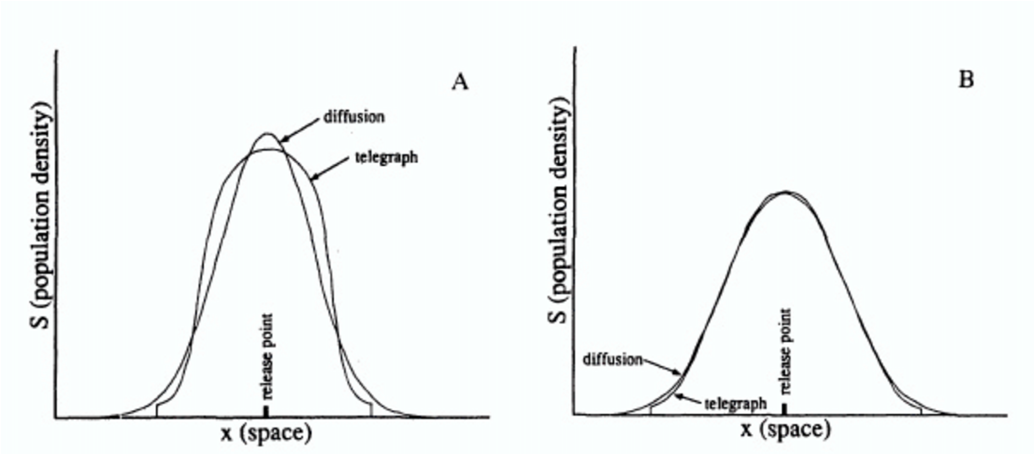

Figure 11: Spatial distribution of a population at different times t_1 (Figure A) and t_2 (Figure B) with $t_1 < t_2$ under the random walk assumption resulting in the diffusion equation and the correlated random walk assumption resulting in the telegraph equation. From [25]

In general, human migration can be described by distributions of the distances between birthplaces of paired persons. If the pairs are spouses, the distribution of matrimonial distances which gives information on the distance of uniting gametes is obtained. If each pair consist of parent and offspring, the distribution of parent-offspring distances which is pertinent for the description of gene migration per generation is derived ([54]). Another possibility is given by the analysis of the exploration range (that is the geographical area which an individual has some probability of visiting in their life time (cf. [24])). Different studies on marriage distances (e.g. [10],[11],[38],[45]) have shown that human dispersal also shows a leptokurtic pattern.

In order to account for the fact of leptokurtic dispersal pattern we generalise our diffusion model (4) by modifying the step length assumption of the random walk model. So far individuals are only allowed to migrate within their neighbourhood and therefore the diffusion model (4) cannot replicate long-range dispersal with plausible values for human mobility. In order to explore the effects of long-range dispersal we allow for step lengths which follow a 'heavy tailed' distribution as shown in Figure 12. In doing so we replace the mathematical description of the diffusion process (the Laplace operator $\triangle$) by a so called dispersal kernel formulation which results (under suitable parameterisation) in leptokurtic dispersal patterns of the population.

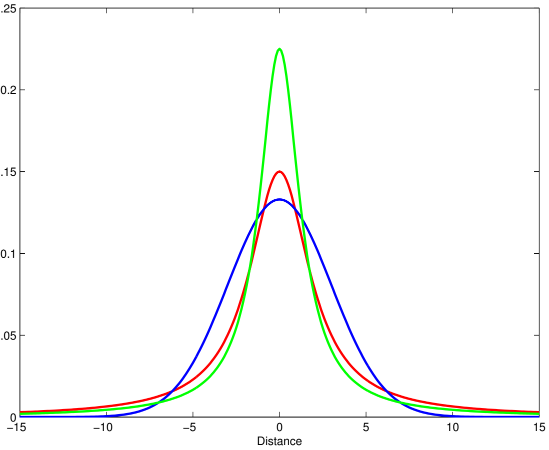

Figure 12: Different distribution functions. The blue line shows the normal distribution ($\mathcal{N}(0,2)$) and the red and green lines Cauchy distributions (which belong to the class of leptokurtic distributions) with the variances 2 and 4 respectively.

Dispersal kernel formulation. So far we assumed that human dispersal can be described by a diffusion process using the locally acting Laplace operator $\triangle$. This implies that individuals interact only within their neighbourhood and therefore the standard diffusion approach (4) cannot replicate very fast demic expansion or long-range dispersal with plausible values for human mobility and reproduction. In order to explore the effects of long-range dispersal on the dispersal dynamic of the population we replace the diffusion term $D\triangle u$ by the integral formulation

$$\lambda \left[\int_D u(t, x+\delta)\varphi(\delta)d\delta - u(t,x) \right].$$

The variable u represents again the space- and time-dependent proportion of the population. The kernel function $\varphi(\delta)$ defines the probability distribution of the dispersal lengths δ. Figure 12 shows examples of such kernels. It is obvious that large dispersal lengths δ are rare but occur with positive probabilities. The coefficient λ can be interpreted as a measure of the dispersal rate. A detailed mathematical review of such dispersal models can be found e.g. in [36],[15].

3 Reaction

After modelling dispersal phenomena we turn our attention to growth processes. Here we understand growth as the increase or decrease of the variable of interest (e.g. population size, number of individuals who use a new technology) due to intrinsic birth-death processes. Similar to diffusion dynamics, where Fick's law provided the fundamental principle growth behaviour can be characterised by a very small number of basic concepts such as the Malthusian or the logistic growth model. The Malthusian law of growth proposes that the human population of a nation grows exponentially (at least for a while). Contrarily, the logistic law postulates that the rate of growth is proportional to both the present population size and the amount of available resources and is therefore bounded if the amount of resources are limited.

In the following we introduce four fundamental growth models

- the exponential growth,
- the logistic growth,
- the confined exponential growth,
- the Gompertz growth

and discuss their mathematical formulation, properties and applicability to different growth situations. The considerations are based on the textbook by Robert B. Banks ([7]).

3.1 Exponential growth function

Thomas R. Malthus (who published one of the earliest and most influential books on population growth: 'An Essay on the Principle of Population') proposed a population growth model which is essentially exponential growth. This means that the growth rate is proportional to the population's current size[11]. The mathematical formulation of the exponential growth model has the form

$$\frac{\partial u}{\partial t}(t) = au(t) \tag{6}$$

where the growth rate $\frac{\partial u}{\partial t}$ describes the temporal change of the population size and a stands for the intrinsic growth coefficient which represents the proportional increase of the population size u per unit of time. The solution of this differential equation is given by

$$u(t) = u_0 e^{at} \tag{7}$$

which describes the growth process of the population over time starting from the initial population size u_0. If the growth coefficient a is positive we observe an increase in population size whereas a negative a implies a decrease in population size. Further, we can derive that for positive growth coefficients a model (6) results in unbounded growth. The growth rate (or in other words the increase of the population size from one time step to the other) is always positive and therefore after a finite time period the magnitude of the population size u goes towards infinity (cf. red dashed line in Figure 14).

This unbounded growth property reduces the applicability of model (6) in practise. Exponential growth models of physical phenomena only apply within limited periods, as unbounded growth is not physically realistic.

---

[11] Very generally the growth rate can be determined from empirical data by calculating the quotient

$$\frac{\text{population size at the end of the period} - \text{population size at the beginning of the period}}{\text{population size at the beginning of the period}}.$$

3.1.1 Applications

- The exponential function is a good model for the growth of the population of the United States in the time period from 1790-1870. After this time period (following the end of the civil war) a crowding effect began to be felt so that there were no circumstances for unbounded growth. This decelerated growth is well described by the logistic equation which we consider in the next section.
- There are many other examples for exponential growth during a short period of time. But because of the property of unboundedness we can not describe a whole growth process with this function.
- A virus (for example SARS, West Nile or smallpox) will typically spread exponentially at first, if no artificial immunization is available. Each infected person can infect multiple new people.
- Nuclear chain reaction (the concept behind nuclear weapons). Each uranium nucleus that undergoes fission produces multiple neutrons, each of which can be absorbed by adjacent uranium atoms, causing them to fission in turn. "Due to the exponential rate of increase, at any point in the chain reaction 99% of the energy will have been released in the last 4.6 generations. It is a reasonable approximation to think of the first 53 generations as a latency period leading up to the actual explosion, which only takes 34 generations." (Sublette, Carey. "Introduction to Nuclear Weapon Physics and Design". Nuclear Weapons Archive. http://nuclearweaponarchive.org/Nwfaq/Nfaq2.html. Retrieved 2010-08-09.)

3.1.2 Gompertz model*

One possibility to construct a more realistic approach is to consider a temporally varying growth rate

$$a(t) = a_0 e^{-kt}$$

where a_0 is a chosen initial value and $k > 0$ the decay coefficient. This results in the well-known Gompertz model which is defined by equation (6) with a exponential decreasing growth rate $a(t)$[12]

$$\frac{\partial u}{\partial t}(t) = a(t)u(t) = a_0 e^{-kt} u(t). \tag{8}$$

In this case the growth dynamic is determined by

$$u(t) = u_0 e^{\left(\frac{a_0}{k}(1-e^{-kt})\right)}. \tag{9}$$

From this equation we can derive the following relationship

$$u(t) = u^\star = u_0 e^{\frac{a_0}{k}} \quad \text{for} \quad t \to \infty. \tag{10}$$

The term $u^\star$ represents the asymptotic value of the population size u for sufficiently long times t and can be seen as a carrying capacity (which can be interpreted as an upper

---

[12] Note, that for $k = 0$ equation (9) reduces to the exponential function (6).

boundary of the population size) but it is not a result of a crowding effect rather than the result of opposite growth directions of both, the growth coefficient a and the population size u. Figure 13 shows the growth dynamic for different values of the coefficient k. It is obvious that the smaller k the higher is $u^\star$ and the more the Gompertz growth resembles the exponential growth model.

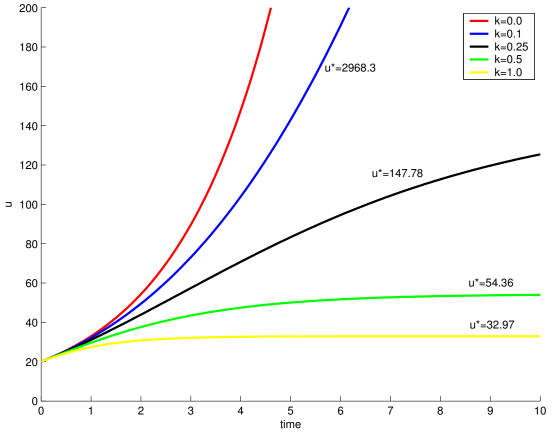

Figure 13: Gompertz curves with $u_0 = 20$, $a_0 = 0.5$

3.2 Logistic growth function

Pierre Franois Verhulst suggested in 1844 a different growth model where the rate of growth is proportional to both the present population size and the amount of available resources. In this way the growth is bounded due to limitation of resources (such as food resources, living space, etc.). The resulting model, the so called logistic growth model, is self-limiting if the population becomes too large. It balances the competing dynamics of exponential growth and environmental limitation.

As in the previous section the variable u describes the population size and the logistic growth model is formalised by the following equation

$$\frac{\partial u}{\partial t} = a\left(1 - \frac{u}{K}\right)u \tag{11}$$

where a is the growth coefficient and K describes the carrying capacity of the environment (an upper boundary for population size ([13]), which is usually determined by the given sustaining resources).

The population dynamic given by the logistic growth model (11) is given by

$$u(t) = \frac{u_0 K e^{at}}{K + u_0(e^{at} - 1)} \quad \text{with the initial population size} \quad u(0) = u_0. \tag{12}$$

Consequently for positive growth coefficients a the population size, whose temporal dynamic is described by equation (12), converges against K for sufficiently large times t. This means the growth is bounded by the carrying capacity K[13].

---

[13] Note that for $K \to \infty$ equation (12) reduces to the case of exponential growth.

If we examine equation (11) more closely we find that in early unimpeded periods where $u \ll K$ holds the growth rate $\partial u/\partial t$ is mainly determined by the first term $+au$. The value of the growth coefficient a represents the proportional increase of the population size u per unit of time. As time progresses and the population size increases, the second term, which multiplied out is $-au^2/K$, becomes more dominant because some members of the population interfere with each other by competing for some critical resource, such as food or living space. This antagonistic effect is called bottleneck, and its strength is modelled by the value of the carrying capacity K. The competition for resources between the members of the population diminishes the growth rate, until the population size u ceases to grow (what is called maturity of the population).

These effects are clearly shown in Figure 14. For every small initial population size $0 < u_0 \ll K$ the population grows initially similar to an exponential growth model (cf. solid and dashed red lines), however, if the population size gets larger the growth rate becomes smaller resulting in a much slower growth. Finally the population size reaches the carrying capacity K and the growth is ceased off. If the initial value u_0 is larger then K the sign of the term $\left(1 - \frac{u}{K}\right)$ changes and the population size decreases until it has reached the size K (cf. the case $u_0 = 150$ in Figure 14).

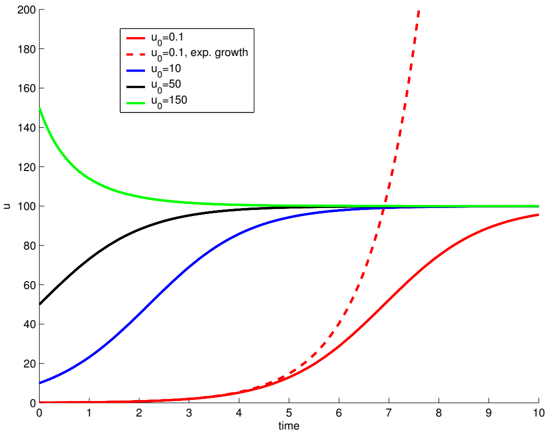

Figure 14: Logistic functions with $u_0 = 0.1; 10; 50; 150$

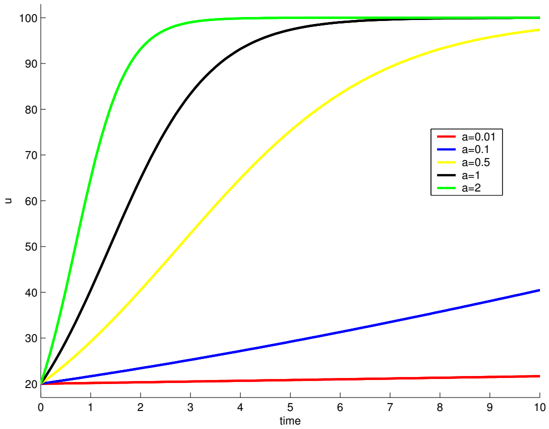

Figure 15: Logistic functions with $a = 0.01; 0.1; 0.5; 1; 2$

Figure 15 shows the influence of the growth coefficient a (assuming $a > 0$) on the growth dynamic. As stated above a represents the proportional increase of the population size u per unit of time and is consequently a measure of how fast the carrying capacity K is reached. It is obvious that the greater the growth coefficient a the faster the equilibrium K is reached.

3.2.1 Applications

In the following we list a number of important applications of the logistic growth model.

- As mentioned in section 3.1 the logistic growth function can be used for describing certain time periods of the development of different human or animal populations.

- Another application of the logistic curve is in medicine, where the logistic differential equation is used to model the growth of tumors.
- In the social learning theory the adoption curve of the spread of an innovation through a population by social learning shows a logistic growth pattern.
- In linguistics, the logistic function is supposed to model language change. An innovation which is marginal at first begins to spread quickly with time and by the end of this process there remains only a very small number of items that did not undergo the change in question.
- The logistic equation (12) can provide an appropriate framework for the analysis and display of data concerning technology substitutions. In terms of the theory of innovation diffusion it can be said: The transfer rate (growth rate) $\frac{\partial u}{\partial t}$ is treated solely as a function of interpersonal communication or social interaction between prior adopters and potential adopters in a social system (cp. [33]). It is a basis for personal, pure interaction mechanism for transfer.

3.3 Confined exponential growth function

We have seen that the logistic growth model is an appropriate framework to describe personal, pure interaction mechanism for the transmission of information. In this context a different growth model, the confined exponential growth, has been proposed to model pure impersonal transmission of information.

The confined exponential growth model is a bounded growth process which can be described by the following equation

$$\frac{\partial u}{\partial t}(t) = a(K - u(t)) = aK - au(t) \tag{13}$$

where a is the growth (or transfer) coefficient and K the carrying capacity. The solution of the equation above, the magnitude of population size at any given point in time, is given by

$$u(t) = K - (K - u_0)e^{-at} \quad \text{with the initial population size} \quad u(0) = u_0 \tag{14}$$

where the population size u approaches K for sufficient long times t. This simple type of exponential growth is always confined to a region bounded by K. The growth dynamic given by equation (14) is illustrated in Figure 16 (solid lines) for different initial population sizes $u_0 = 0.1; 10; 50; 150$, a carrying capacity $K = 100$ and a growth coefficient $a = 1.0$. It is obvious that as time progresses the population size converges toward the carrying capacity K. Figure 17 shows the influence of the coefficient a on the growth dynamic. As in the case of logistic growth we obtain that the greater the growth coefficient a the faster the equilibrium K is reached. However, if we compare the logistic growth dynamic given by equation (12) with the dynamic of the confined exponential growth given by equation (14) (cf. dotted and dashed red lines). While the logistic growth resembles exponential growth for small population sizes u (which is characterised by small growth rates for small population size due to assumed proportionality between growth rate and current population size) confined exponential growth has its maximum growth rates for small population sizes u. It is often stated in the literature that logistic growth leads to an S-shaped growth curve whereas confined exponential growth leads to a r-shaped growth curve.

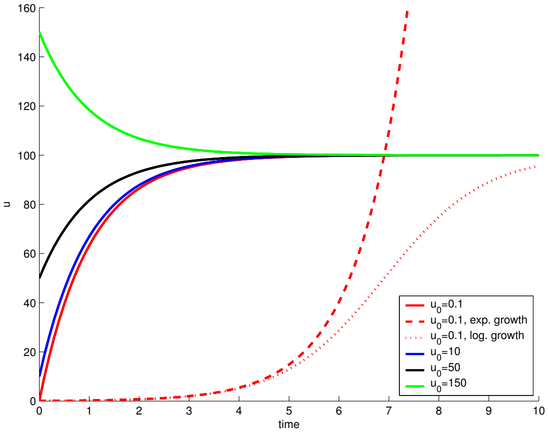

Figure 16: Confined exponential functions with $u_0 = 0.1; 10; 50; 150$

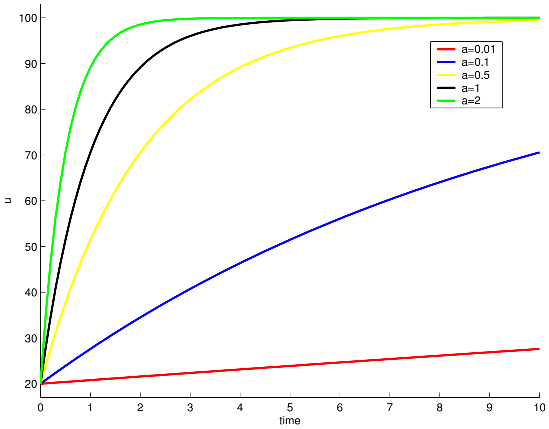

Figure 17: Confined exponential functions with $a = 0.01; 0.1; 0.5; 1; 2$

3.3.1 Applications

- In contrast to the logistic equation (12) the considered confined exponential equation can be a model for a impersonal, pure source mechanism for transfer of innovations. In that context the constant a is defined as a measure of external influence emanating from outside the social system, e.g. the effect on mass media communication (cp. [33]). The model does not contribute to any interactions within the population and therefore it is only applicable if e.g. adequate information about the innovation is only available from a source external to the social system.
- In the social learning theory adoption curves of the spread of an innovation through the population resulting from asocial learning are mainly r-shaped.

4 Diffusion-reaction systems

After considering different approaches for describing dispersal and growth phenomena separately we now study the population dynamic obtained by combining both mechanisms. We allow the population to grow and to disperse at the same time and are interested in the temporal and spatial behaviour of the population size under different growth models (exponential growth, logistic growth, confined exponential growth, Gompertz growth). We analyse so called diffusion-reaction systems of the form

$$\frac{\partial u}{\partial t}(t,x) = D \triangle u(t,x) + f(u). \tag{15}$$

where the time- and space dependent function u again describes the population size at any location x and time t. The temporal change of the population size at location x is given by the diffusion component $D\triangle u(t,x)$ and the growth component $f(u)$. We will see that depending on the chosen growth model we obtain very different population dynamics.

For the solution (that means an analytic expression of the function $u(t,x)$ which describes the population size at every location x and time t) of such partial differential equations we need to specify initial and boundary conditions. We assume that we are only interested in the behaviour of the population in a bounded domain D and therefore define equation (15) only over the domain D. The considered domain can be of almost any shape. We set the following initial condition

$$u(0,x) = u_0, \quad x \in \overline{\mathsf{D}}$$

which defines the population size at time $t = 0$ in the considered domain and the boundary condition

$$u(t,x) = 0, \quad x \in \partial\mathsf{D}$$

which defines the behaviour of the population at the boundary. In this case we assume that no member of the population can occupy the boundary $\partial\mathsf{D}$, the population size is zero at all times t. There are other possibilities for defining boundary conditions. E.g. we can assume

$$\frac{\partial u}{\partial n}(t,x) = 0, \quad x \in \partial\mathsf{D}$$

what means there is no diffusion possible beyond the boundary ∂D. This assumption would be fulfilled if we imagine D as isolated by natural barriers, preventing exchange with the wider world.

4.1 Diffusion-reaction system with exponential growth

In the case of the exponential growth model the population dynamic is described by

$$\frac{\partial u}{\partial t}(t,x) = D \triangle u(t,x) + au(t,x). \tag{16}$$

In the following we will consider the population dynamic on a rectangular area D but for the sake of better visualisation we will only analyse the spread and growth process along a cut through the area, that means along a line.

Figure 18 shows the spatial distribution of the population (based on equation (16 with the parameters $D = 10$ and $a = 1.0$) along the line for different times.

At time $t = 0$ the population is assumed to be uniformly distributed in a small area (cf. Figure 18a). Then time progresses, growth and dispersal occurs and Figures 18b-d show the population dynamic at different times $t_1 < t_2 < t_3$. Remembering the properties of the exponential growth function it is not surprising that the density grows unboundedly and after a finite time the whole domain D is occupied (cf. Figures 18b-d). However, we see that due to the chosen boundary condition the population size is always zero at the boundaries.

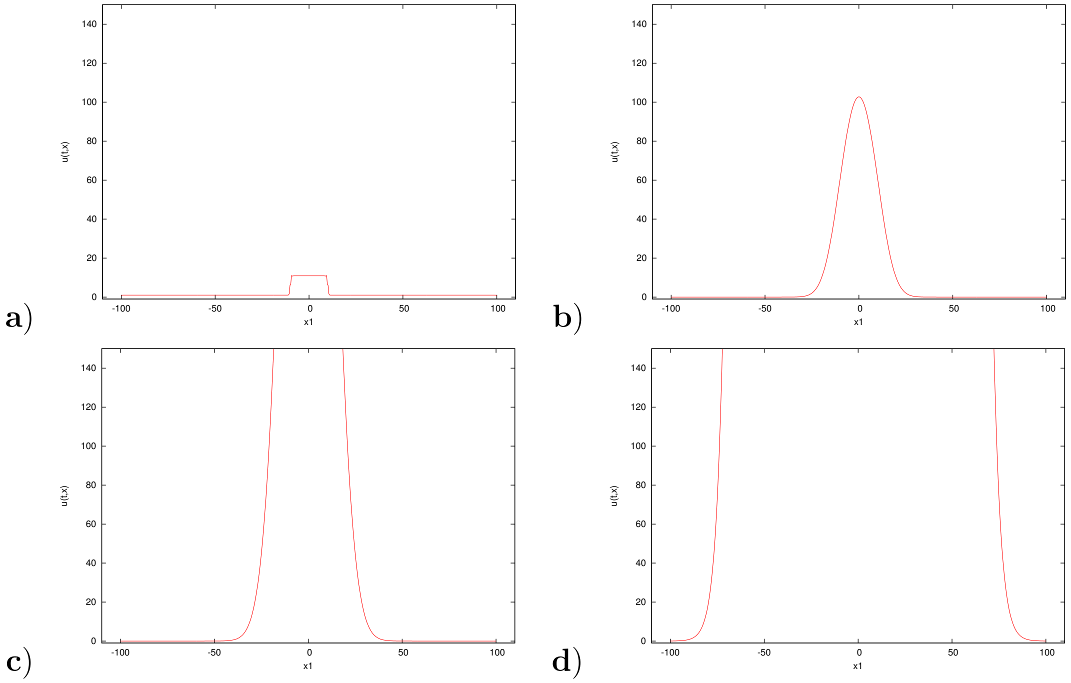

Figure 18: Population density at different times t_0, t_1, t_2 t_3

4.2 Diffusion-reaction system with logistic growth

By far the most widely used dispersal-growth model is obtained by modelling the growth component in equation (15) as a logistic growth process. We obtain

$$\frac{\partial u}{\partial t}(t,x) = D \triangle u(t,x) + au(t,x)\left(1 - \frac{u(t,x)}{K}\right). \tag{17}$$

Analogous to the case of exponential growth consider the obtained population dynamics (for the same parameter values $D = 10$ and $a = 1.0$) at the times $t_0 < t_1 < t_2 < t_3$. Further, the carrying capacity (the upper limit of the population size) K is set to be 100. Initially the population is uniformly distributed in a small area (cf. Figure 19a). Now time progresses and diffusion and growth occurs. As the initial population size is smaller than the carrying capacity the population grows until the K is reached which happens roughly at time t_1 (cf. Figure 19b). Now the spatial spread pattern of the population can be described as a travelling wave (cf. grey boxes in Figures 19b-d). We see that once the wave front is formed it does not change its shape as time progresses.

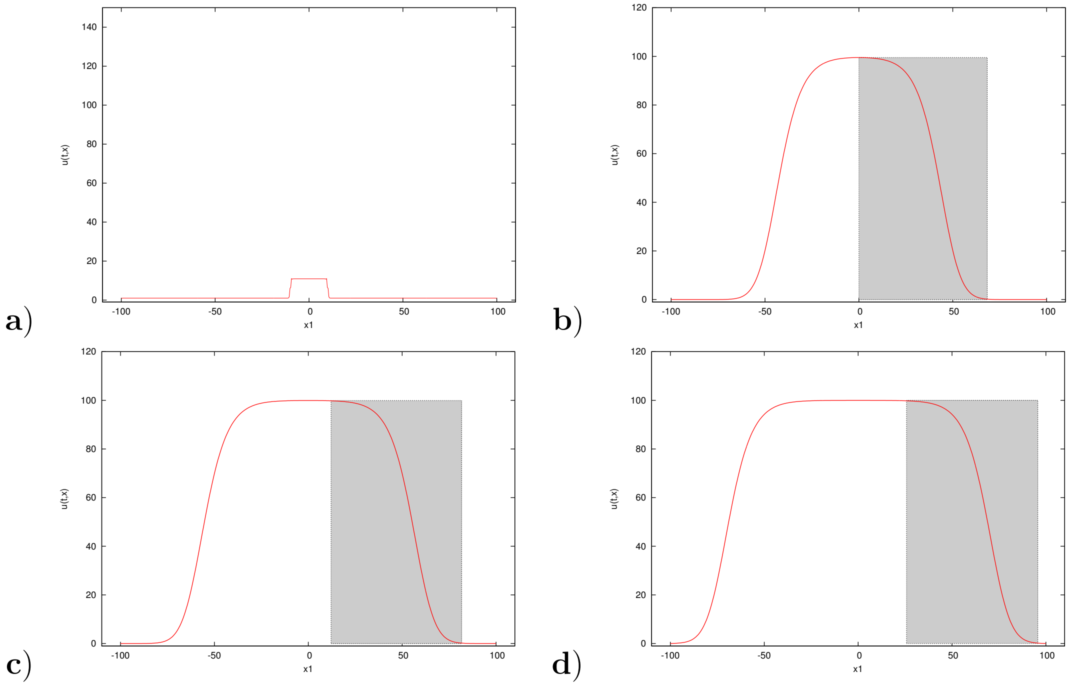

Figure 19: Population density at different times t_0, t_1, t_2 t_3

It can be shown that the wave front (the grey boxes in Figures 19b-d), over which the population changes from a high to a low density is dependent on the diffusivity D and the growth coefficient a and it holds the following relationship for the wave width

$$\xi \sim \sqrt{D/a}.$$

We can immediately derive that small values of a relative to those of D correspond to large transition regions (or wave widths), and contrary small values of D relative to those of a correspond to small transition regions (or wave widths). Another important characteristic for describing population dispersal is the speed with which the wave travels. It can be shown that the wave speed ν is also dependent on a and D. It holds

$$\nu = 2\sqrt{Da}.$$

The higher the diffusivity D and/or the growth coefficient a the faster the wave travels.

Estimation of the parameter D and a. If applied to human dispersal the diffusivity D represents the degree of mobility of an individual (e.g. [3]). In general individuals will move from their birthplace a distance λ during their generation time τ. The square of this distance will in general be proportional to the time available; the constant of proportionality is the diffusion constant D

$$D = \lambda^2/4\tau.$$

A good proxy of this distance λ is the marriage distance. The growth coefficient a is comparable easy to estimate. The quotient

$$\frac{\text{population size at the end of the period} - \text{population size at the beginning of the period}}{\text{population size at the beginning of the period}}$$

gives us an estimate for au/K. By adjusting for u/K we obtain the desired growth rate a.

4.2.1 Applications

- Equation (17) is also known as the Fisher-Kolmogoroff equation. Fisher suggested this model in [17] as a model for the spatial spread of a favored gene in a population. In this context the coefficient a is a measure for the benefit induced by this gene.

- Many human dispersal phenomena are described using equation (17) (cf. the spread of hunter-gatherers into North America, spread of agriculture)

4.3 Diffusion-reaction system with confined exponential growth

In this section we assume the confined exponential growth model and describe the dispersal-growth process of the population by

$$\frac{\partial u}{\partial t}(t,x) = D \bigtriangleup u(t,x) + a\left(K - u(t,x)\right).$$

We assume the same model parameter as before ($D = 10$, $a = 1$, $K = 100$) and again start with a population which is uniformly distributed over an small area at time $t = 0$ (cf. Figure 20a). With the first time step the part aK of the reaction term $a(K - u(t,x))$ acts on the whole domain D and causes the population size to be instantaneously increased over the whole domain (cp. Figures 20b-d). Due to the properties of the confined exponential growth the population grows until the carrying capacity K is reached.

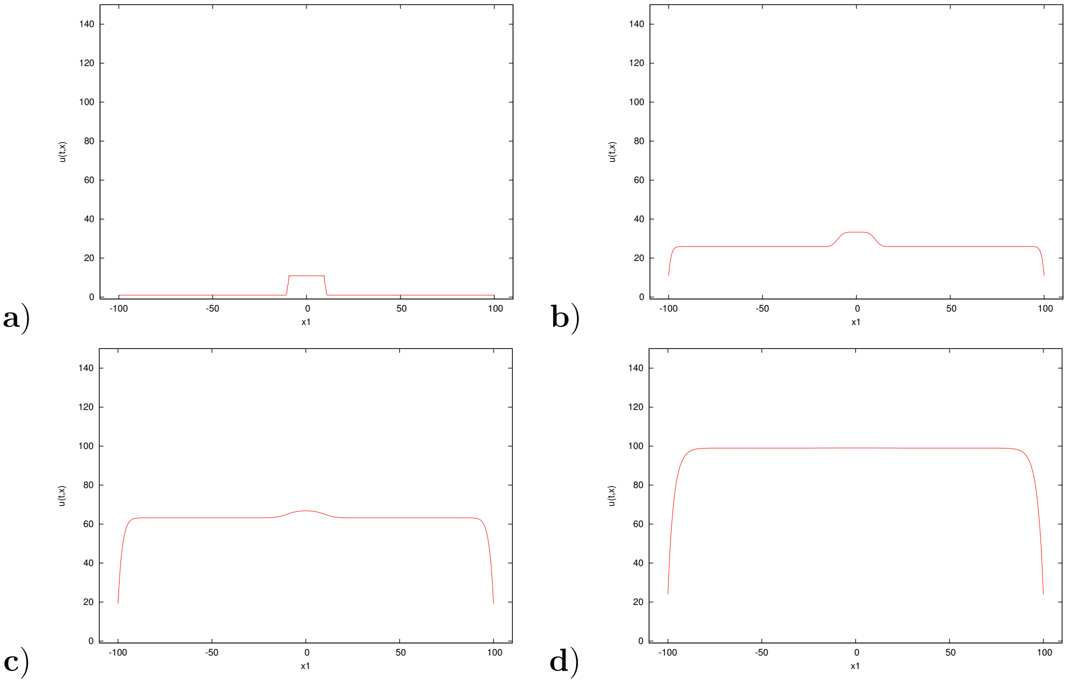

Figure 20: Population density at different times t_0, t_1, t_2 t_3

These Figures illustrate nicely that the confined exponential growth function is a model for impersonal, pure source mechanism for transfer of innovations and is not a model for any interactions within the population.

4.4 Diffusion-reaction system with Gompertz growth

Lastly we consider the impacts of the Gompertz model on the population dynamic by analysing the equation

$$\frac{\partial u}{\partial t}(t,x) = D \triangle u(t,x) + a_0 e^{-kt} u(t,x).$$

Again we use the same parameter constellation ($D = 10$, $a = 1$) as in the previous sections and set $k = 0.3107$, so according to equation (10) the intrinsic carrying capacity of the Gompertz growth function has the value 100. Starting off with a population initially uniformly distributed over a small area (cp. Figure 21a) we obtain an interesting dynamic as time progresses (cf. Figures 21b-d).

The population grows but the growth coefficient $a(t) = a_0 e^{-0.3107t}$ decreases exponentially and at a certain time $\bar{t}$ the diffusion is “stronger” than the reaction. The diffusion causes dispersal of the population and that’s why the intrinsic carrying capacity $u^\star = 100$ (cp. equation (10)) for the Gompertz growth function will not be reached (see Figure 21b). After the time $\bar{t}$ the effect of the diffusion is obvious - the population spreads out and the reaction or growth term is negligibly small (see Figure 21d).

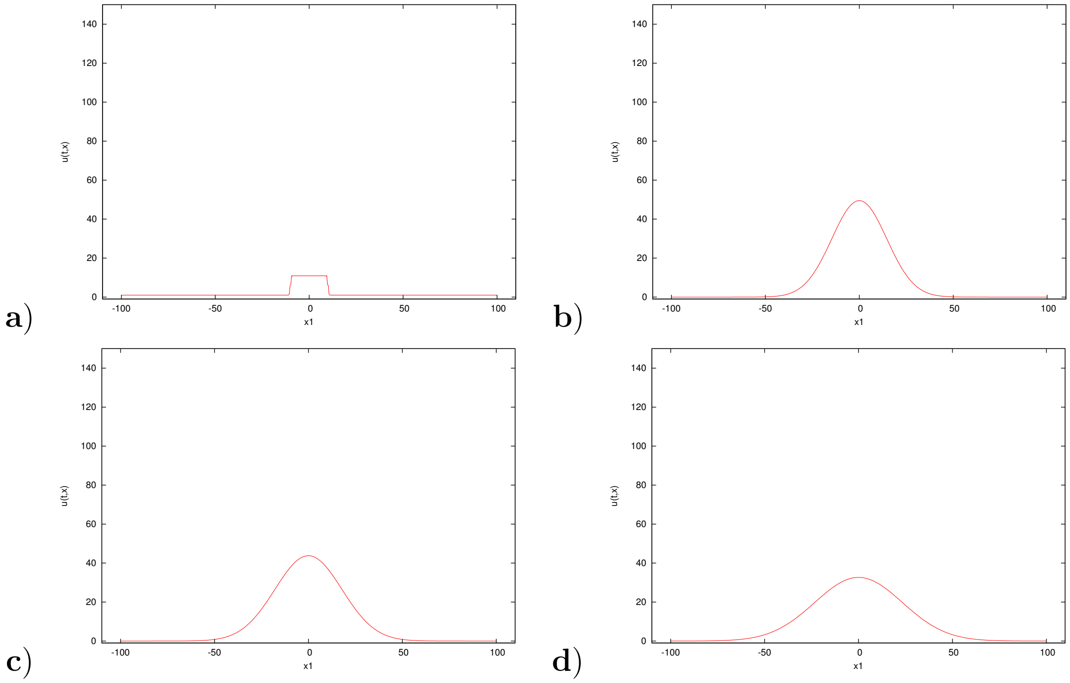

Figure 21: Population density at different times t_0, t_1, t_2 t_3

5 Interaction between dispersing populations

So far we focused on describing the dispersal pattern of a single population in an unoccupied habitat. But what happens if the dispersing population comes into contact with other populations? Depending on the kind of interaction one would expect significant changes in the dispersal patterns. Very generally interactions can be divided into three groups ([41])

- **Prey-predator interactions:** If the growth rate of one population is increased but decreased for the other then we are in a predator-prey situation.
- **Competition:** If the presence of the other population decreases the growth rate for both populations then we are in a competition situation.
- **Mutualism:** If each population's growth rate is enhanced then it's called mutualism.

In this section we study how those interactions can be modelled and describe their influence on the population dispersal dynamic. The first and very influential approaches of modelling population interactions go back to V. Volterra and A. Lotka who independently derived equations to describe the dynamics of interacting species in an ecological context[14]. They showed that the simplest of ecosystems, involving only a predator and

---

[14] While Volterra ([52]) derived this model to explain the oscillatory levels of certain fish catches in the Adriatic Lotka ([31]) derived the equations from a hypothetical chemical reaction which exhibited periodic behaviour in the chemical concentration ([41]).

prey species, could go through endless cycles of changing population size as the growth of the prey population produces an increase in the predator population. That in turn leads to a decline in the prey population, which is followed by a decline in the predator population. Interestingly S. Levin quotes that "Volterra's greatest contribution was not his specific equations, but rather in the heterodox idea that sophisticated mathematical methods could be used to understand the dynamics of natural systems"([30]).

In the following we analyse the prey-predator and competition situation in more detail. For consideration of mutualism we refer to [41].

5.1 Prey-Predator models

When predators are successful at catching prey they will reproduce more reliably and their species will increase in numbers whereas the numbers of their prey will fall. However, the larger predators population will struggle to find enough food to support them and their numbers will fall because of the reduced population of prey species. Eventually the situation will reverse itself as the number of prey increase due to less predation. If the ecosystem is large enough and other factors do not have an excessive effect, this can result in a situation in which populations of predator and prey rise and fall at regular intervals, with a small time lag between them. This dynamic is described mathematically by the following Lotka-Volterra system

$$\begin{aligned}\frac{\partial N}{\partial t} &= N(a - bP) \\ \frac{\partial P}{\partial t} &= P(cN - d).\end{aligned} \tag{18}$$

The time-dependent variables N and P stand for the population sizes of the prey and predator population, respectively, and the terms $\partial N/\partial t$ and $\partial P/\partial t$ define the temporal change in frequency of both populations. In the absence of any predators (that means $P = 0$) the prey grows exponentially, modelled by the term aN ($a > 0$). So the coefficient a is the intrinsic growth rate of the prey population if no interactions with the predator population occur. The effect of predation is to reduce the growth aN by the term $-bPN$ ($b > 0$) which is proportional to both, the prey and the predator population. In the absence of any prey (that means $N = 0$) the predator population is reduced exponentially which is modelled by the term $-dP$ ($d > 0$). Lastly the predators growth is dependent on the availability of prey and therefore is modelled by the term cPN ($c > 0$). Figure 22 shows exemplified a solution of system (18). We see clearly the described cyclic pattern in the prey and predator population over time and the small time gap between both cycles. Naturally the prey reaches its peak first.

Figure 23 shows a real-life example of prey-predator interactions. It illustrates data on Canadian lynx-snowshoe hare interactions in the fur catch records of the Hudson Bay Company from about 1845 until the 1930s. It is assumed that the numbers reflect a fixed proportion of the total population of these animals. Although this assumption is questionable the data represent one of the few long term records available. We clearly see the periodic behaviour of both population sizes and also the time gap between the cycles.

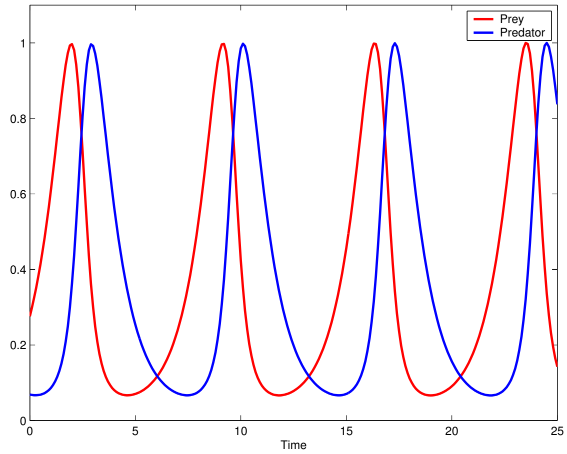

Figure 22: Example of the time course of a prey and predator interaction.

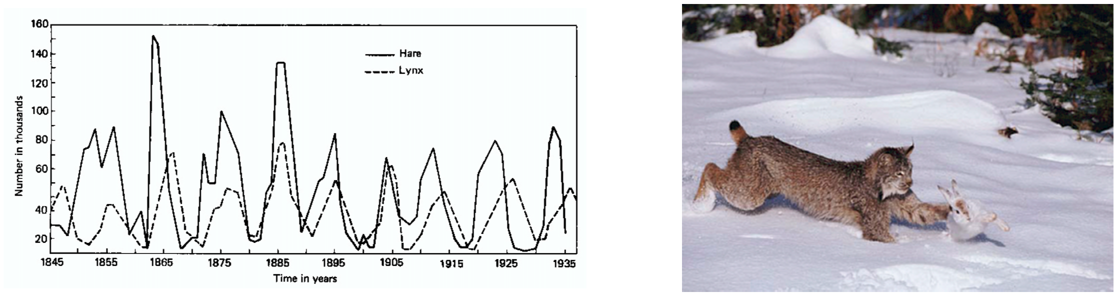

Figure 23: (left) Changes of the abundance of the lynx and the snowshoe hare, as indicated by the number of pelts received by the Hudson's Bay company. Redrawn from [43] (right) Prey-predator interaction (www.nationalforestlawblog.com)

However, the introduced Lotka-Volterra model has some serious shortcomings that reduce its applicability. The solutions of system (18) (as exemplarily shown in Figure 22) are not structurally stable meaning that very small perturbations of the system can result in a significant change at least in the amplitude of the oscillations. The solution is not robust against small changes/uncertainties in the model parameters. This is caused by unrealistic assumptions (such as the unbounded prey growth in absence of predators).

Generalisation of the Lotka-Volterra system. To address the mentioned shortcoming and to obtain a structurally stable solution we follow [41] and generalise approach (18) to

$$\begin{aligned}\frac{\partial N}{\partial t} &= NF(N,P)\\ \frac{\partial P}{\partial t} &= PG(N,P)\end{aligned}$$

where the particular form of the functions F and G depends on various factors such as the kind of interactions, the interacting species, etc. A reasonable choice for F is

$$r\left(1-\frac{N}{K}\right)-PR(N)$$

where the growth of the prey population in absence of predators shows a logistic pattern and is therefore bounded by the carrying capacity K. Further, the predation term $PR(N)$ which is a functional response of the predators to changes in the prey density is assumed to be bounded, too ([41]). Hence we replaced the predation term bNP in the Lotka-Volterra model (18) by the bounded expression $PNR(N)$. The function G can be modelled by

$$G(P,N)=k\left(1-h\frac{P}{N}\right).$$

Here the carrying capacity (a measure for the maximum population size) of the predators is directly proportional to the prey density ([41]).

5.2 Competition models

Not all populations show a prey-predator relationship. In this section we consider situations where two or more species compete for some limiting resource. This limiting resource can be food or nutrients, space, mates, nesting sites, in general anything for which demand is greater than supply. The pure presence of a competitor, or even more extreme if the competitor has an advantage in exploiting the resources, will negatively affect the growth rate of the population. This naturally influences the population dynamics of the competitor, too.

The competition dynamic between two populations can be described by the following model

$$\begin{aligned}\frac{\partial u_1}{\partial t} &= d_1\triangle u_1+a_1u_1\left(1-\frac{u_1}{K_1}-c_1\frac{u_2}{K_1}\right)\\ \frac{\partial u_2}{\partial t} &= d_2\triangle u_2+a_2u_2\left(1-\frac{u_2}{K_2}-c_2\frac{u_1}{K_2}\right)\end{aligned} \qquad (19)$$

where u_1 and u_2 stand for the frequencies of population 1 and 2, respectively. Spatial dispersal is modelled by the diffusion processes $d_i\triangle u_i$ where d_i describes the diffusivity of both populations (meaning the rate at which both populations move to areas which are not occupied by this population). In the absence of the other population (either $u_1 = 0$ or $u_2 = 0$ in the whole considered area) system (19) reduces to equation (17). The interactions between the populations are defined by the competition terms $c_1 u_2/K_1$ and $c_2 u_1/K_2$. The constants c_i, $i = 1, 2$ define the competition coefficients representing the influence of the competitor on the growth of each population i. The higher the competition coefficient c_i the more is the growth of population i restricted by the presence of the other population. The outcome of the competition is either coexistence between the two populations or competitive exclusion (which means that one population will go extinct in the long run). Which of both possible outcomes is reached is determined by the carrying capacities K_i (defining the upper boundary of the respective population size) and the competition coefficients c_i. We obtain coexistence if it yields

$$c_1 < K_1/K_2 \quad \text{and} \quad c_2 < K_2/K_1$$

([42]). Figure 24 shows an example of the coexistence situation where population 1 (red lines) has a slight competitive advantage. We start with a spatial distribution of both populations as illustrated in Figure 24a, so both populations are initially separated. Now time goes on, dispersal and growth occurs and both populations come into contact. They interact and due to the competitive advantage of population 1 it is able to establish itself at a higher frequency, however both populations coexist (cf. Figure 24d).

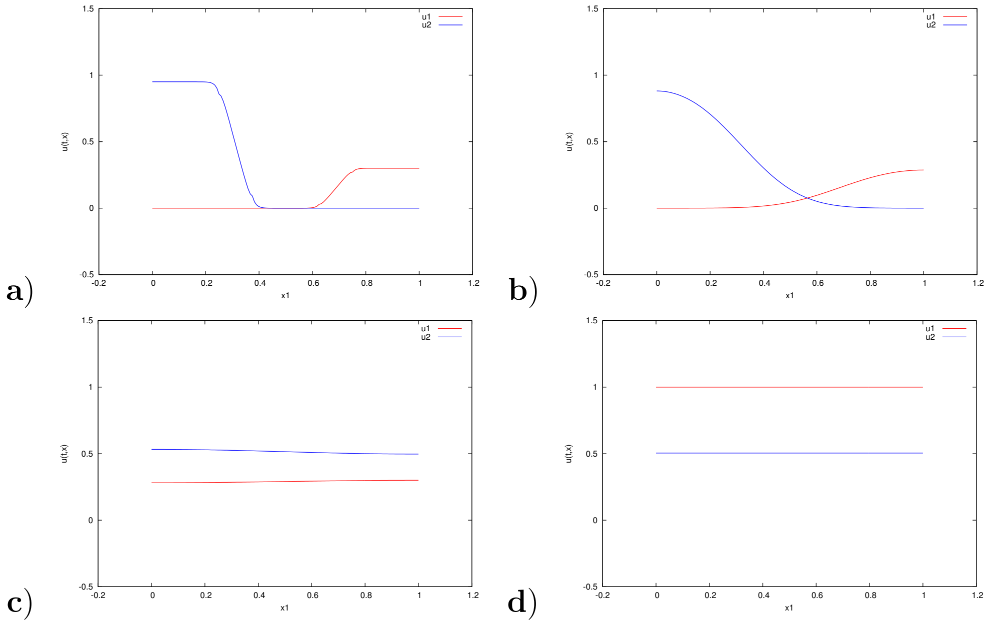

Figure 24: Densities at different times t_0, t_1, t_2 t_3 for population 1 (red lines) and population 2 (blue lines)

Contrary, competitive exclusion is reached if it holds

$$c_j > K_j/K_i \quad \text{and} \quad c_i < K_i/K_j$$

(with population j going extinct). Further, if it yields

$$c_1 > K_1/K_2 \quad \text{and} \quad c_2 > K_2/K_1,$$

then eventually one population will go extinct, but which one depends on the initial frequencies ([42]). Figure 25 shows an example of the extinction situation. We assume the same situation as in Figure 24 but increase the competitive advantage of population 1 (that means decrease c_1 and/or increase c_2). We observe that now coexistence is no longer possible. The presence of population 1 in the same domain drives population 2 to extinction (cf. Figure 25d).

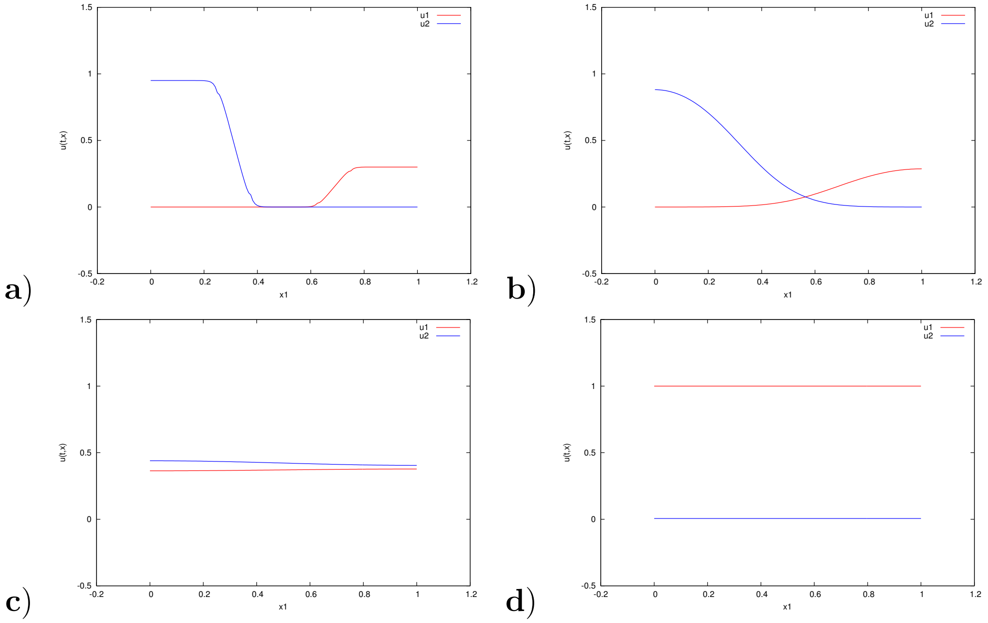

Figure 25: Densities at different times t_0, t_1, t_2 t_3 for population 1 (red lines) and population 2 (blue lines)

Remark 2. In many-real world applications (especially if we consider the spread of competing cultural traits) the competition terms are actually shift terms $c_1 u_1 u_1/K_1 = c u_1 u_2/K$ and $c_2 u_1 u_1/K_2 = -c u_1 u_2/K$. That means the gain of one population is the loss of the other. Further, we assumed so far that both populations have their own carrying capacity K_1 and K_2 which is a realistic assumption when we consider the interactions between different species. In this context the carrying capacities represent the maximum population sizes of species that an area can support without reducing its ability to support the same species in the future ([13]). But in the cases where we consider the competition between two populations of the same species that happen to carry two different cultural traits (examples of those traits are language, life style, ethnicity, etc.) the assumption of two separate carrying capacities is not appropriate. So unless socioeconomic factors create entirely separate niches for each cultural trait and its speakers, there should be only one upper boundary for population size, the maximum number of individuals which is supported by a given area, regardless of the carried cultural trait. Here we introduce the concept of a common carrying capacity K. That means that the frequencies of individuals carrying cultural trait 1 (our population 1) and cultural trait 2 (our population 2) have to fulfill the condition

$$u_1 + u_2 \leq K,$$

where K stands for the common carrying capacity. This condition changes the growth dynamics of both languages even in the absence of competition. Assuming u_2 is fixed then the frequency of population 1 must be less than or equal to $K - u_2$ so that the condition $u_1 + u_2 \leq K$ is met. In other words, the population sizes u_1 and u_2 can grow only until (respectively) $K - u_2$ and $K - u_1$ are reached. That leads to modified logistic growth functions of the form

$$a_1 u_1 \left(1 - \frac{u_1}{K - u_2}\right) \quad \text{and} \quad a_2 u_2 \left(1 - \frac{u_2}{K - u_1}\right).$$

Generalisations of this model have been applied e.g. to problems of language shift (e.g.[1], [47],[37],[28]) or to model the interactions between Neolithic farmers and mesolithic hunter-gatherers ([4],[5]).

5.2.1 Language shift

In this section we briefly demonstrate how competition models are applied to describe the phenomenon of language shift. We define language shift as the process where members of a community in which more than one language is spoken abandon their original vernacular language in favour of another. Membership of a community defined by its language selectively facilitates and inhibits interaction, enables entry into social contracts and co-operative exchange, and gives access to a reservoir of accumulated and linguistically-encoded knowledge. In cases of language contact, therefore, people are inevitably confronted with difficult choices about which language they wish or need to speak. The major driver of language shift is the decision to abandon a more local or less prestigious language, typically because the target of the shift is a language seen as more modern, useful, or giving access to greater social mobility and economic opportunities ([34],[8],[39]).

In [28] we model the dynamics of language shift as a competition process in which the numbers of speakers of each language vary as a function both of internal recruitment (as the net outcome of birth, death, immigration and emigration rates of native speakers), and of gains and losses due to language shift. That means we examine the dynamics of language shift as a spatially-dependent competitive process using the reaction-diffusion system

$$\begin{aligned}
\frac{\partial u_1}{\partial t} &= d_1 \triangle u_1 + a_1 u_1 \left(1 - \frac{u_1}{K - (u_2 + u_3)}\right) - c_{13} u_1 u_3 + c_{12} u_1 u_2 \qquad (20) \\
\frac{\partial u_2}{\partial t} &= d_2 \triangle u_2 + a_2 u_2 \left(1 - \frac{u_2}{K - (u_1 + u_3)}\right) + c_{13} u_1 u_3 + c_{31} u_1 u_3 \\
&\qquad - c_{12} u_1 u_2 - c_{32} u_2 u_3 \\
\frac{\partial u_3}{\partial t} &= d_3 \triangle u_3 + a_3 u_3 \left(1 - \frac{u_3}{K - (u_1 + u_2)}\right) - c_{31} u_1 u_3 + c_{32} u_2 u_3
\end{aligned}$$

with the boundary conditions $\partial u_i / \partial n = 0$, $x \in \partial D$, $i = 1, 2, 3$ where $\partial / \partial n$ is the outer normal derivation. The time- and space-dependent variables u_1 and u_3 stand for the frequencies of monolingual speakers of Language A and Language B respectively, whereas u_2 describes the frequency of bilingual speakers of both languages. The terms $\partial u_i / \partial t$,

$i = 1, 2, 3$ indicate the rate of change in these frequencies over time. The terms on the right hand side of the equations in system (20) describe the changes in frequency of speakers in each of the three subpopulations u_1, u_2 and u_3. The components $a_i u_i(1 - u_i/(K-(u_j+u_k))$ define the internal reproductive rates, which represent coupled biological and cultural reproduction within each sub-population. This is usually modelled (as shown here) as a logistic process with intrinsic rate of increase a_i. The variable K stands for the carrying capacity of the environment and defines an upper limit to the size of the whole population regardless of the languages spoken, which imposes the condition $u_1+u_2+u_3 \leq K$ for any time t (i.e. we assume that our human sub-populations must compete for a common resource base). The mobility of speakers of each sub-population in space within the modelled region is modelled by the diffusion terms $d_i \triangle u_i$. The language shift dynamic is modelled in system (20) by the frequency-dependent conversion term $c_{ij} u_i u_j$. The coefficients c_{13} and c_{31} represent the likelihood of language shift causing speakers to become bilingual based on the differential prestige or attractiveness of the two competing languages. Following ([37]) we assume $c_{13} = \tilde{c}_{13}(1 - s)$ and $c_{31} = \tilde{c}_{31} s$ where the variable s describes the social status differences between the two languages on a scale from 0 to 1. The higher the status of a language the higher is the likelihood of being the preferred target of shifting. The coefficients $\tilde{c}_{13}$ and $\tilde{c}_{31}$ model the likelihood that monolinguals will respond to these status differences by learning the other language. Language shift cannot happen by passing directly from being monolingual in one language to being monolingual in the other language, but must involve a bilingual transition state (cf. Figure 26). The bilingual sub-population therefore recruits from both monolingual sub-populations at a rate $(c_{13} + c_{31})u_1 u_3$. In turn, bilinguals shift to being monolingual in one or other language at a rate $c_{12} u_1 u_2$ (representing the loss to monolingualism in Language A) and $c_{32} u_3 u_2$ (representing the loss to monolingualism in Language B). The coefficients c_{12} and c_{32} represent the likelihood of bilingual speakers then becoming monolingual in each of the two languages. In real life this transition back to monolingualism happens when bilingual parents choose to raise their children monolingually, or when speakers reared as bilinguals in bilingual households abandon one of their languages during their lifetime. We define the overall balance of competitive advantage to speaking each language on the base of the conversion rates: for example, fluency in Language A can be assumed to be more advantageous if it holds that $c_{31} < c_{13}$ and $c_{12} > c_{32}$. This implies that when the monolingual sub-populations are compared, monolinguals of Language A are less likely to become bilingual, and bilinguals are more likely to shift to speaking only Language A.

Model (20) shift leads inevitably to the extinction of one or other monolingual sub-population, followed by the extinction of the language itself in the bilingual community. However, extinction may not always be the fate of the lower-status language. The lower-status language can prevail, provided that its speakers have an initial numerical advantage that outweighs their languages intrinsic status disadvantage. In formal terms, and if overall population size is stable, this outcome requires that there are initially few enough monolinguals in the high-status language, and enough pressure on them to become bilingual, for it to always hold that $c_{12} u_2 > c_{31} u_3$.

This model has been successfully applied to the Gaelic-English competition in Western Scotland (cf. [28]). The historical shift to English by Gaelic speakers of Scotland is a particularly well-studied example of language competition, for which good census data exists for the most recent 100-120. Figure 27 (solid lines) shows the change in the pro-

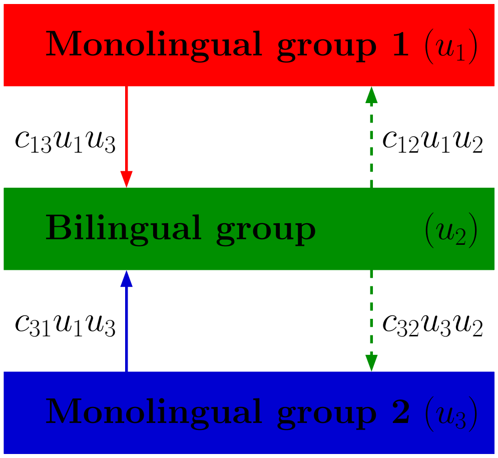

Figure 26: Scheme of the assumed language shift dynamic.

portions of monolingual English- and Gaelic-speakers and bilinguals for the counties of Argyll, Inverness, Ross & Cromarty and Sutherland during the time period 1891-1971. These four counties are seen as the 'core land' of the Gaelic language ('Gaidhealtachd'): in 1891 73% of all Scotland's Gaelic speakers were located among the 8% of Scotland's population that lived in these 'Highland Counties', covering the mainland Highlands and the Western Isles. It is obvious (cf. dashed lines in Figure 27) that our basic model (20) captures the general dynamic of the past language shift process well (the decrease of the Gaelic- and Welsh-monolingual and bilingual sub-populations and the increase of the English-monolingual sub-population).

In order to use model (20) to make predictions about the future shift pattern we need to assume that the cultural environment is unchanged. However, this has not been true in the Gaelic-English competition situation. Recent revitalisation efforts have included the establishing of Gaelic-medium pre-school and primary school units ([32]) and the development of Gaelic-medium broadcasting ([40]). In 2005 the Gaelic Language (Scotland) Act was passed by the Scottish Parliament, providing a planning framework for a number of additional shift reversal measures, while Comhairle nan Eilean Siar, the Western Isles Council, has adopted Gaelic as its primary language. Summarising, interventions have been undertaken in order to improve the status and the presence of the Gaelic language in Scotland and therefore the competition environment has been altered. To model the effects of planned interventions we generalise in [28] the basic language shift model (20) by incorporating a simplified concept of (extended) diglossia. While in the majority of social domains the shift mechanisms of the basic model apply, diglossia pertains to some restricted social domain in which the balance of competitive advantage differs from that which drives the main shift process. Analysis of our diglossia model has shown (cf. [28]) that the key language planning issues for maintenance of an endangered language are

- to create or support social domains in which the endangered language is the preferred or only acceptable medium of communication, and
- to increase the rate of intergenerational transmission of the endangered language.

Other important dimensions of language maintenance are the creation of economic in-

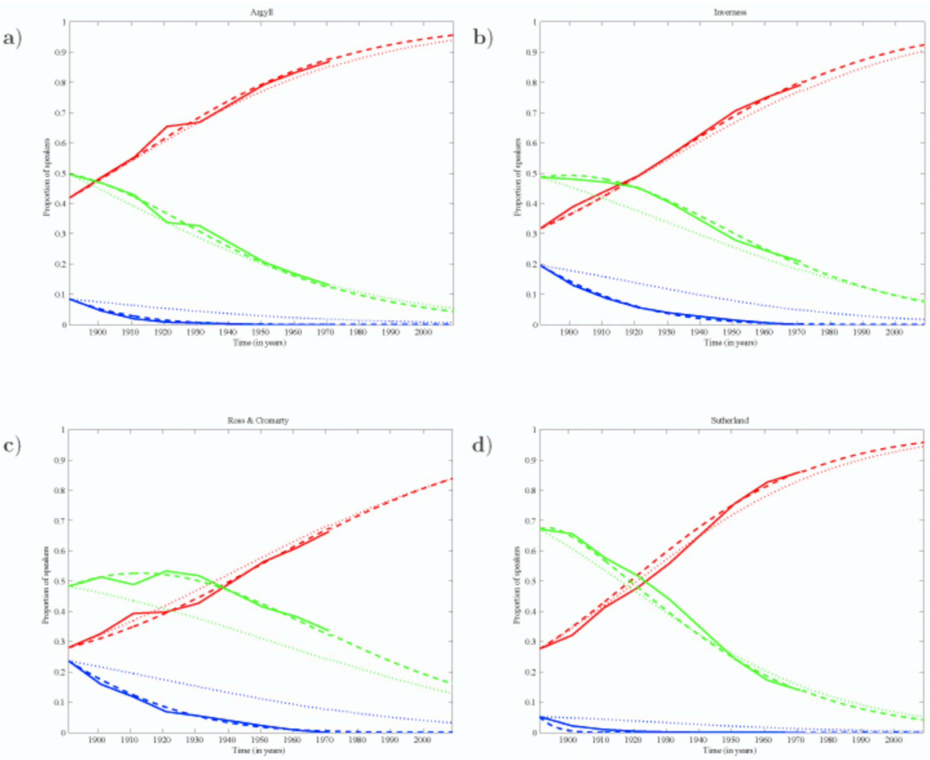

Figure 27: . Frequencies of the three sub-populations in the four Scottish Highland counties for the time period 1891-2010. Empirical data (solid lines) and predictions of model (1) under the assumptions $c_{31} = c_{32}$ and $c_{13} = c_{12}$ (dotted lines) and $c_{31} \neq c_{32}$ and $c_{13} \neq c_{12}$ (dashed lines) of the frequencies of Gaelic (blue), bilingual (green) and English (red) speakers in Argyll (a), Inverness (b), Ross & Cromarty (c), Sutherland (d) over time.

centives (e.g. jobs created to implement language planning-related initiatives and which themselves require skills in the endangered language), and the establishment of corpora of written texts in the endangered language as a cultural archive and as a medium of continuing cultural self-expression. Without stabilizing a sustainable level of intergenerational transmission, language planners will have to rely on constant interventions in formal public domains (e.g. in the school curriculum) to counter the continuing outflux from bilingualism by individual households. An indication of one cause of this background outflux from Gaelic-speaking bilingualism can be found in the 2001 Scottish census data (Registrar General for Scotland (2005)): 70% of children aged 3-15 years speak Gaelic in households in which a married or co-habiting couple both speak Gaelic, while the percentages are only 18% if the male partner alone speaks Gaelic, and 27% if the female partner alone speaks Gaelic. This is the current reality of intergenerational transmission in an environment where languages compete with very unequal external advantages.

6 Documentation of the 'CultDiff' software package

We have seen in the last sections that diffusion-reaction models are powerful tools for modelling dispersal processes. However, we have also seen that in order to apply this framework we need to solve a differential equation or even a system of differential equations. So contrary to agent-based simulations the application of the diffusion-reaction approach requires some advanced mathematical knowledge.

To make this approach useable to a broader audience we started the open software project 'CultDiff'. The aim of this software package is to determine the solution of problems such as e.g. (17) or (19) under specific assumptions for the model parameter or the shape of the considered domain. 'CultDiff' uses GNU Octave (a free software primarily intended for numerical calculations which can be downloaded under www.gnu.org/software/octave/download.html)[15], however, the implementation of the mathematical solution technique itself is done in C++. A flow chart (cf. Figure 28) demonstrates the succession of the various program steps. The red squares stand for Octave/MatLab parts which can be manipulated by the user, the green square characterises the 'CultDiff' core program (which carries out all necessary calculation step) and the blue squares indicate the data flow between both parts.

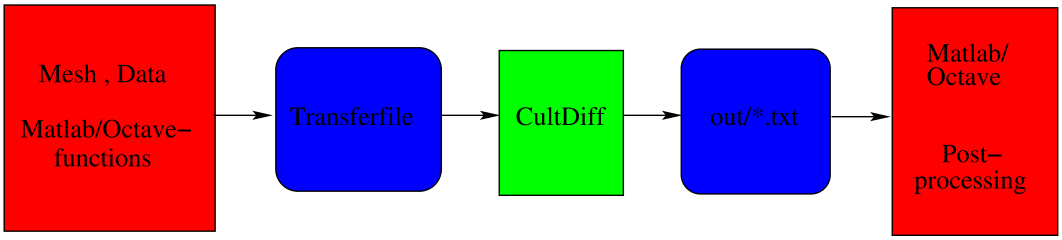

Figure 28: 'CultDiff' - Workflow

The heart of 'CultDiff' is the implementation of the Finite Element Method (FEM) which is a numerical procedure that enables us to find approximate solutions of partial differential equations or systems of partial differential equations. The Finite Element Method envisions the considered domain $\mathbb{D}$ as built up of many small, interconnected subregions or finite elements (such as triangles) and the basic idea of the method is that a considered domain $\mathbb{D}$ can be approximated by replacing it with an assemblage of finite elements. So a finite element solution gives a piecewise approximation to the original problem.

The discretisation of the domain $\mathbb{D}$ into finite elements is one crucial element of the theory. Figure 29 shows exemplarily the discretisation of a rectangular domain into triangles. The starting point is always the description of the domain geometry (in our case simply the rectangle) and the coarsest triangulation of the domain (in our case two triangles, cf. Figure 29 (left)). In every discretisation or refinement step each triangle will be subdivided into four triangles and after four refinement steps the rectangle possesses a discretisation as shown in Figure 29 (right). The discretisation procedure is automated in 'CultDiff'. The user only needs to provide the description of the domain geometry and its coarse

---

[15] Of course if MatLab is available 'CultDiff' can be used in exactly the same way.

discretisation. It is important to note at this point that the finer the discretisation the more accurate is the solution. However, a higher level of refinement of course increases the calculation effort and therewith the calculation time. So the trick is to find a balance between fast computation and accurate results.

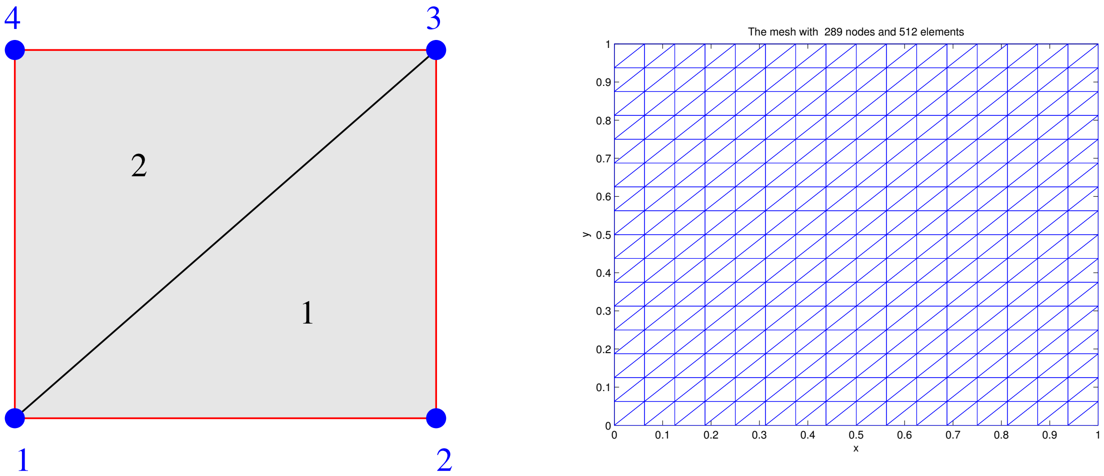

Figure 29: (left) The initial discretisation of a rectangle (right) and the obtained discretisation after four refinement steps.

6.1 Dispersal of one population

We demonstrate now the use of 'CultDiff' step by step on the following reaction-diffusion problem with logistic growth (cf. section 4.2)

$$\frac{\partial u}{\partial t}(t,x) = D \triangle u(t,x) + au(t,x)\left(1 - \frac{u(t,x)}{K}\right) \qquad x \in \mathbb{D} := [0,1] \times [0,1]$$

with the boundary condition

$$\frac{\partial u}{\partial n}(t,x) = 0, \qquad x \in \partial\mathbb{D}$$

and the initial condition (that means the distribution of the population at time $t = 0$)

$$u(0,x) = u_0(x) := \begin{cases} 0.9 & \text{if} \quad \sqrt{x_1^2 + x_2^2} < 0.2 \\ 0.0 & \text{otherwise.} \end{cases}$$

Further, the model parameters are set as follows

$$D = 10^{-5}, \ a = 0.01, \ K = 1.$$

With the setting $K = 1$ the variable $u(t,x)$ can be interpreted as the proportion of the carrying capacity K which has been 'used' by the population at time t and in location x. In order to pass these parameter values on to the 'CultDiff' program we need to modify four m-files which handle the definition of the model parameter:

- `get_initialcondition.m` for defining the initial condition,
- `get_diffusion.m` for defining the diffusivity D,
- `get_growth_coefficient.m` for defining the growth coefficient a,
- `get_competition.m` for defining logistic growth and the carrying capacity.

6.1.1 `Get_initialcondition.m`

The function `get_initialcondition.m` defines the spatial distribution of the population at the beginning of the consideration. In our example was assume a spatial distribution as shown in Figure 30.

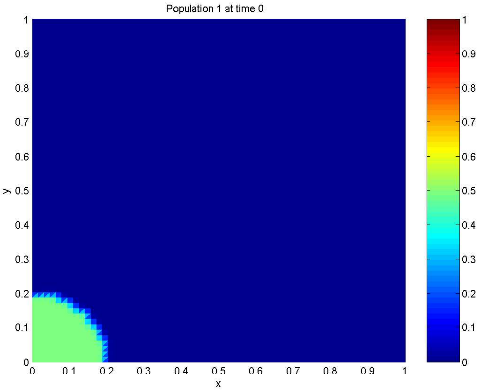

Figure 30: Spatial distribution of the population at time $t = 0$

We assume that the population is present in a circular area with the center point (x_m, y_m) and the radius r. These values and the actual population size u_0 at time $t = 0$ must be chosen by the user (see red lines below).

```
%--------------------------------------------------------------
%Population 1
%--------------------------------------------------------------
%Definition of the region where the population 1 is present initially
%Circle with midpoint xm,ym and radius r
xm = 0.0;
ym = 0.0;
r = 0.2;
ftest = (x-xm)^2 + (y-ym)^2 - r^2;
if ( (p==1) & (ftest <0 ) )
u0=0.5;
end;
```

6.1.2 `Get_diffusion.m`

In this file the values of the diffusivity D of the population over the whole domain $\mathbb{D}$ are defined. In our case we assume that D has the constant value of 10^{-5} over the whole domain. All we need to do is to input the desired value for D in the red highlighted line.

```
%------------------------------------------------------------------
%Population 1
%------------------------------------------------------------------
% set the default diffusivity for population 1
if ( p==1 )
D=1.0e-5;
end;
```

However, some applications may require that the diffusivity varies across the considered domain (e.g. populations will spread slower in mountain regions than in lowlands). 'Cult-Diff' enables the user to define regions where the diffusivity D differs from the value set as the default value (cf. red line above). If we assume e.g. that in an elliptic region the diffusivity is reduced to 10^{-6} then we need to define the region where the diffusivity differs and set D accordingly. This can be easily done by uncommenting (that means deleting the % sign) and modifying the already prepared code:

```
% the center points
xm = 0.6
ym = 0.4
% the half axes, a in x direction, b in y-direction
a = 0.4
b = 0.2
% rotating angle
phi = 30
% Computation of the ellipse
x1=x-xm;
y1=y-ym;
%Rotation
c=cos( phi*pi/180);
s=sin( phi*pi/180);
x= c*x1 + s* y1;
y= -s*x1 +c* y1;
ftest = x*x/(a*a) + y*y/(b*b) -1; if ( (p==1) & (ftest <0 ) )
D=1.0e-6;
end;
```

Thereby the parameter (x_m, y_m) define the center point of the ellipse and a, b the length of the half axes (cf. Figure 31). The angle φ defines how much the ellipse is inclined to the right (cf. Figure 31).

Additional shapes (such as circle or rectangle) are pre-defined in `Get_diffusion.m` and can be used in a similar way. The definition of multiple areas is of course also possible.

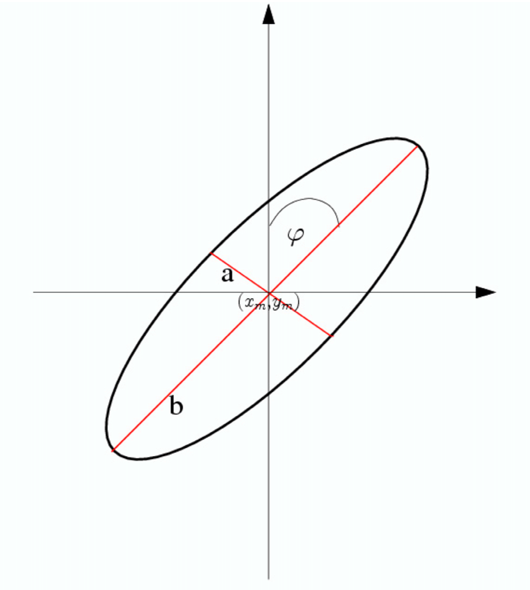

Figure 31: Positioning of the ellipse

6.1.3 `Get_growth_coefficient.m`

The file `get_growth_coefficient.m` defines the growth coefficient over the whole domain $\mathbb{D}$. Here we assume $a = 0.01$ (see red line below).

```
%---------------------------------------------------------------
%Population 1
%---------------------------------------------------------------
%set default growth coefficient population 1
if ( (pi==pj) & (pi==1) )
a=0.01;
end;
```

Spatially variable growth coefficients can be defined in a similar manner as described in section 6.1.2 and examples are already included in the file.

6.1.4 `Get_competition_coefficient.m`

Here we define whether we assume logistic or exponential growth and the carrying capacity. If we set the variable `log_growth` to 1 we assume logistic growth and contrary for 0 we assume exponential growth.

```
% log_growth = 1 for logistic growth and log_growth = 0 for exponential growth
log_growth = 1;
%Definition of the carrying capacity
K=1;
```

6.1.5 Running 'CultDiff'

After we have set the parameter values the only thing left to do is to specify the finite element parameter. To do that we modify the file param.txt.

```
%   Model Parameters
%
1     % number of populations
1.0   % time step length tau
900   % maximal number of time steps
4     % number of domain refinement steps
```

We consider the spread of one population only and therefore the number of populations is 1. The time-step size τ determines the step size of the numerical time-step-method. The default value is 1 so that we can interpret all results as per one month, year, generation, etc. The definition of this time step length has implication for the model parameter estimation. They always have to estimated per time step length. The maximal number of time steps defines the total time period of the simulation (in our case 900 years). And lastly the number of domain refinements define the level of discretisation of our domain (cf. Figure 29).

Now we are finally ready to go. To run the 'CultDiff' please follow the following steps.

1. Open Octave/MatLab.
2. Change into the subdirectory Example.
3. Type `cultdiff_run` into the Octave/MatLab command window.

During the run of the programm all output-information will be written to the subdirectory `out`. For each time step a txt-file containing the values of $u(t,x)$ in discrete locations/nodes x_i (the finer the chosen discretisation the shorter is the distance between neighbouring nodes x_i) is produced. For a visualisation of the solution we use the file `cultdiff_post` (simply type `cultdiff_post` into the Octave command window) which creates a plot of the solution $u(t,x)$ at a given time step over the whole domain $\mathbb{D}$. In order to set the time step: open the file `cultdiff_post.m` and set the variable `step` at the desired value

```
% the timestep to plot
step=100;
```

Figure 32 shows the solution of our diffusion-reaction system with logistic growth at time $t = 900$ for two different refinement levels. It is obvious the finer is the discretisation the smoother is the solution.

With the help of Octave/MatLab much more postprocessing steps, like time-dependent plots, animations, parameter estimations for wave speeds are possible. The only needed input are the values of $u(t,x)$ at times t and locations x (which are saved in the corresponding data files in the output-directory).

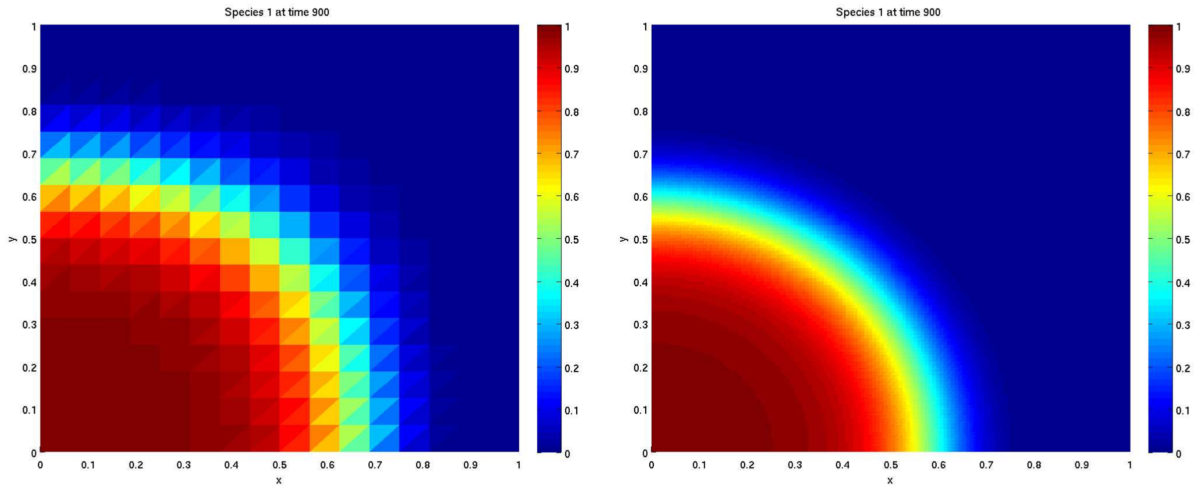

Figure 32: (left) The solution $u(t,x)$ at time $t = 900$ if the domain has been discretised three time (512 elements) and (right) the solution $u(t,x)$ at times $t = 900$ if the domain has been discretised five times (32768 elements)

6.1.6 Definition of the geometry

So far we used a simple rectangular domain for our considerations. However, the domain $\mathbb{D}$ can be of almost any geometric structure. This structure is defined in the files `mesh-nodes.txt` and `mesh-elements.txt` . The node file `mesh-nodes.txt` contains the geometric information about the domain $\mathbb{D}$ by defining appropriate nodes (which are given by their x- and y-coordinate and their node number). The element connectivity file `mesh-elements.txt` defines the coarse triangulation of the considered domain $\mathbb{D}$. Each triangle is determined by its three corner points. For a good approximation these triangles must fulfill some conditions, especially they must cover the whole domain D and the triangles must not overlap. For the rectangular domain both files are defined as follows

`mesh-nodes.txt`

```
% nodelist for rectangle [0,1]x[0,1]
% x - y coordinates of node 1..N
0.0 0.0 (point 1 in Figure 29 (left))
1.0 0.0 (point 2 in Figure 29 (left))
1.0 1.0 (point 3 in Figure 29 (left))
0.0 1.0 (point 4 in Figure 29 (left))
```

`mesh-elements.txt`

```
% element-connectivity table for rectangle [0,1]x[0,1]
% every line stands for the 3 node numbers which define the triangle
1 2 3 (triangle 1 in Figure 29 (left))
1 3 4 (triangle 2 in Figure 29 (left))
```

For more complex geometries we must adjust these two files. Exemplarily we show this for the domain shown in Figure 33.

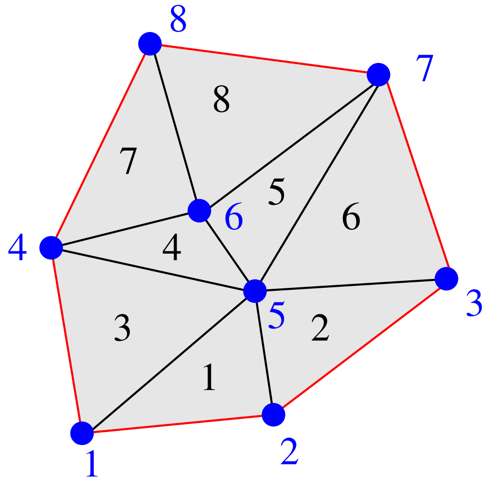

Figure 33: A triangular finite element mesh

In order to obtain a triangulation of the domain we add two points (4 and 5 in Figure 33) to the 'corner' points $\{1, 2, 3, 4, 7, 8\}$. This is necessary because otherwise we cannot describe the whole considered domain by non-overlapping triangles. The geometry files read like follows:

`mesh-nodes.txt`

```
% nodelist
% x - y coordinates of node 1..N
0.0 0.0 (point 1 in Figure 33 )
1.0 0.2 (point 2 in Figure 33 )
2.0 0.8 (point 3 in Figure 33 )
-0.1 1  (point 4 in Figure 33 )
0.9 0.7 (point 5 in Figure 33 )
0.6 1.2 (point 6 in Figure 33 )
1.7 1.8 (point 7 in Figure 33 )
0.4 2.0 (point 8 in Figure 33 )
```

`mesh-elements.txt`

```
% element-connectivity table
% every line stands for the 3 node numbers which define the triangle
1 2 5 (triangle 1 in Figure 33 )
2 3 5 (triangle 2 in Figure 33 )
1 5 4 (triangle 3 in Figure 33 )
4 5 6 (triangle 4 in Figure 33 )
5 6 7 (triangle 5 in Figure 33 )
5 3 7 (triangle 6 in Figure 33 )
4 6 8 (triangle 7 in Figure 33 )
6 7 8 (triangle 8 in Figure 33 )
```

6.2 Dispersal of and competition between two populations

In this section we demonstrate the use of 'CultDiff' for competition models (cf. section 5.2)

$$\begin{aligned}\frac{\partial u_1}{\partial t} &= d_1 \triangle u_1 + a_1 u_1 \left(1 - \frac{u_1}{K_1} - c_1 \frac{u_2}{K_1}\right)\\ \frac{\partial u_2}{\partial t} &= d_2 \triangle u_2 + a_2 u_2 \left(1 - \frac{u_2}{K_2} - c_2 \frac{u_1}{K_2}\right)\end{aligned}$$

with the boundary conditions

$$\frac{\partial u_i}{\partial n}(t,x) = 0 \quad i = 1,2, \qquad x \in \partial\mathbb{D}$$

and the initial conditions (that means the distribution of the populations at time $t = 0$)

$$u_1(0,x) = u_{1,0}(x) := \begin{cases} 0.9 & \text{if} \quad \sqrt{x_1^2 + x_2^2} < 0.2 \\ 0.0 & \text{otherwise} \end{cases}$$

and

$$u_2(0,x) = u_{2,0}(x) := \begin{cases} 0.9 & \text{if} \quad \sqrt{(x_1-1)^2 + (x_2-1)^2} < 0.2 \\ 0.0 & \text{otherwise.} \end{cases}$$

Further, the model parameters are set as follows

$$D_1 = 10^{-5},\ D_2 = 10^{-4},\ a_1 = 0.02,\ a_2 = 0.01,\ c_{12} = 0.01,\ c_{21} = 0.02,\ K = 1.$$

Again we need to pass these parameter values on to the 'CultDiff' program and therefore modify the four m-files:

- `get_initialcondition.m` for defining the initial conditions,
- `get_diffusion.m` for defining the diffusivities D_1 and D_2,
- `get_growth_coefficient.m` for defining the growth coefficients a_1 and a_2,
- `get_competition.m` for defining logistic growth, carrying capacities and the competition coefficients c_{12} and c_{21}.

We follow the same procedures as described in the previous section with the only difference that we need to define the initial condition, diffusivity and growth coefficient for the second population, too. But that is already pre-defined in the four files.

6.2.1 `Get_competition_coefficient.m`

Beside the decision between logistic and exponential growth and the definition of the carrying capacity the file `get_competition_coefficient.m` defines also the coefficient coefficients c_{12} and c_{12}. All we need to do is to insert the desired values for the competition coefficients (see the red lines below).

```
% Definition of the competition coefficients
c12 = 0.01;
c21 = 0.02;
if ( (e==1 ) & ( pi==1 ) & ( pj ==2 ) ) gamma = -c12; end;
if ( (e==2 ) & ( pi==1 ) & ( pj ==2 ) ) gamma = -c21; end;
```

Spatially variable competition coefficients can be defined in a similar manner as described in section 6.1.2 and examples are already included in the file.

6.2.2 Run 'CultDiff'

The last step is to modify param.txt to

```
%   Model Parameters
%
2     % number of populations
1.0   % time step length tau
900   % maximal number of time steps
4     % number of domain refinement steps
```

and then we can run 'CultDiff' and plot the solutions $u(t, x)$ in the already described way.

Finally, if you use 'CultDiff' (in the current form or your own personal modified form) in an academic publication, please cite this manuscript.

References

[1] D.M. Abrams and S.H. Strogatz. Modelling the dynamics of language death. *Nature*, 424:900, 2003.

[2] A.J. Ammerman and L. L. Cavalli-Sforza. Measuring the rate of spread of early farming in europe. *Man*, 6:674–688, 1971.

[3] A.J. Ammerman and L. L. Cavalli-Sforza. *The Neolithic Transition and the Genetics of Populations in Europe.* 1984.

[4] K. Aoki and M. Shida. Travelling wave solutions for the spread of farmers into a region occupied by hunter-gatherers. *Theoretical Population Biology*, 50:1–17, 1996.

[5] G.J. Auckland, M. Signitzer, and K. Stratford. Cultural hitchhiking on the wave of advance of beneficial technologies. *Proc. Natl Acad. Sci. USA*, 104:8714–8719, 2007.

[6] L. Bachelier. *Théorie de la spéculation.* numdam (France), http://www.numdam.org/item?id=ASENS_1900_3_17__21_0, 1900.

[7] R.B. Banks. *Growth and Diffusion Phenomena.* Springer-Verlag, 1994.

[8] M. Brenzinger. Language maintenance and shift. *in: Keith Brown (ed.) The Encyclopedia of Language and Linguistics (2nd. edition), Vol. 6, Raj Mesthrie (ed.) Society and Language. Oxford: Elsevier*, pages 542–548, 2006.

[9] R.S. Cantrell and C. Cosner. *Spatial Ecology via Reaction-Diffusion Equations.* John Wiley & Sons, Ltd, 2003.

[10] L.L. Cavalli-Sforza. The distribution of migration distances : Models, and application to genetics. *Les diplacements humanis, Entretien de Monaco en Sciences Humainos (ed. T. Suttor)*, pages 139–158, 1961.

[11] D.A. Colemann. The marriage geography in britain, 1920-1960. *Annals of Human Biology*, 4(2):101–132, 1977.

[12] T. Dobzhansky and S. Wright. Genetics of natural populations x. dispersion rates in drosophila pseudoobscura. *Genetics*, 28:304–340, 1943.

[13] P.R. Ehrlich. Ecological economics and the carrying capacity of the earth. *In: Jansson, A. M. Investing in natural capital: the ecological economics approach to sustainability, Island Press*, pages 38–56, 1994.

[14] A. Einstein. Über die von der molekularkinetischen Theorie der Wärme geforderte Bewegung von in ruhenden Flüssigkeiten suspendierten Teilchen. *Annalen der Physik*, 322(8):549–560, 1905.

[15] S. Fedotov. Front propagation into an unstable state of reaction-transport systems. *Physical Review Letters*, 85(5):926–929, 2001.

[16] A. Fick. Über Diffusion. *Annalen der Physik*, 170(1):59–86, 1855.

[17] R.A. Fisher. The wave of advance of advantageous genes. *Ann. Eugenics*, 7:353–369, 1937.

[18] J. Fort, T. Pujol, and L. L. Cavalli-Sforza. Paleolithic population waves of advance. *Cambridge Archaeol. J.*, 14:53–61, 2004.

[19] D.F. Fraser, J.F. Gilliam, M.J. Daley, A.N. Le, and G.T. Skalski. Explaining leptokurtic movement distributions: Intrapopulation variation in boldness and exploration. *The American Naturalist*, 158(2):124–135, 2001.

[20] S. Goldstein. On diffusion by discontinous movements and on the telegraph equation. *Journal of Mechanicsand Applied Mathematics*, 4(2):129–156, 1951.

[21] M. J. Hamilton and B. Buchanan. Spatial gradients in clovis-age radiocarbon dates across north america suggest rapid colonization from the north. *Proc. Natl Acad. Sci. USA*, 104(15):625,630, 2004.

[22] L. Hazelwood and J. Steele. Spatial dynamics on human dispersal: Constraints on modelling and archaeological validation. *Journal of Archaeological Sciences*, 31:669–679, 2004.

[23] J. Henrich. Cultural transmission and the diffusion of innovations: Adoption dynamics indicate that biased cultural transmission is the predominant force in behavioral change. *Am. Antropol.*, 103:992–1013, 2001.

[24] B. Hewlett, J.M.H. van de Koppel, and L.L. Cavalli-Sforza. Exploration ranges of aka pygmies of the central african republic. *Man*, 17(3):418–430, 1982.

[25] E.E. Holmes. Are diffusion models too simple? a comparison with telegraph models of invasion. *The American Naturalist*, 142(5):779–795, 1993.

[26] R. A. Housley, C. S. Gamble, and M. Street et al. Radiocarbon evidence for the late glacial human recolonization of northern europe. *Proc. Prehist. Soc.*, 63:25–54, 1997.

[27] A. Kandler and J. Steele. Social learning, economic inequality, and innovation diffusion. *In Innovation in Cultural Systems: Contributions from Evolutionary Anthropology, M. OBrien and S. Shennan, eds. Cambridge, MA: MIT Press*, pages 193–214, 2009.

[28] A. Kandler, R. Unger, and J. Steele. Language shift, bilingualism and the future of britain's celtic languages. *Phil. Trans. R. Soc. B*, 2010.

[29] A. Kolmogorov, I. Petrovsky, and N. Piscoundov. Etude de l' equation de la diffusion avec croissance de la quantit de matière et son application a un probleme biologique. *Moscow University Bulletin of Mathematics*, 1, 1937.

[30] S. A. Levin. The evolution of ecology. *The chronicle of higher education*, August 8th, 2010.

[31] A.J. Lotka. *Elements of Physical Biology.* Williams & Wilkins, Baltimore, 1925.

[32] K. MacKinnon. Scottish gaelic today: Social history and contemporary status. *In: The Celtic Languages, M.J. Ball ed. London: Routledge*, pages 491–535, 2006.

[33] V. Mahajan and R.A. Peterson. *Models for Innovation diffusion.* SAGE UNIVERSITY PAPER, 1985.

[34] A. McMahon. *Understanding language change.* Cambridge University Press, 1994.

[35] P. Mellars. A new radiocarbon revolution and the dispersal of modern humans in europe. *Nature*, 439:931–935, 2006.

[36] V. Mendez, T. Pujol, and J. Fort. Dispersal probability distributions and the wavefront speed problem. *Physical Review E*, 65(4):1–6, 2002.

[37] J.W. Minett and W.S.-Y. Wang. Modelling endangered languages: The effects of bilingualism and social structure. *Lingua*, 118:19–45, 2008.

[38] R.L. Morrill and F.R. Pitts. Marriage, migration and the mean information field: A study in uniqueness and generality. *Annals of the Assiciation of American Geographers*, 57(2):401–422, 1967.

[39] S. Mufwene. Colonisation, globalisation, and the future of languages in the twenty-first century. *Int. Journal on Multicultural Societies*, 4(2):162–193, 2002.

[40] S. Murdoch. *Language politics in Scotland.* A.U.S.L.Q, 1996.

[41] J.D. Murray. *Mathematical Biology I: An Introduction.* Springer-Verlag, 3rd edition, 2002.

[42] C. Neuhauser. Mathematical challenges in spatial ecology. *Notices Ams. Math. Soc.*, 48:1304–1314, 2001.

[43] E.P. Odum. *Fundamenatals of Ecology.* Saunders, Philadelphia, 1953.

[44] A. Okubo and S.A. Levin. *Diffusion and Ecological Problems: Modern Perspectives.* Springer-Verlag, 2nd edition, 2001.

[45] E. Paradis, S.R. Baillie, and W.J. Sutherland. Modelling large-scale dispersal distances. *Ecological Modelling*, 151:279–292, 2002.

[46] E. Paradis, S.R. Baillie, W.J. Sutherland, and R.D. Gregory. Patterns of natal and breeding dispersal. *Journal of Animal Ecology*, 67:518–536, 1998.

[47] M. Patriarca and T. Leppnen. Modeling language competition. *Physica A*, 338:296–299, 2004.

[48] E.M. Rogers. *Diffusion of Innovations.* 1995.

[49] J.G. Skellam. Random dispersal in theoretical populations. *Biometrika*, 38:196–218, 1951.

[50] J. Steele. Human dispersals: mathematical models and the archeological record. *Hum. Biol.*, 81(2-3):121–140, 2009.

[51] J. Steele, J. Adams, and T. Sluckin. Modeling paleo-indian dispersals. *World Archaeol.*, 30:286–305, 1998.

[52] V. Volterra. Variations and fluctuations of the number of individuals in animal species living together. *J. Cons. Perm. Int. Ent. Mer.*, 3:3–51, 1926.

[53] M. von Smoluchowski. Zur kinetischen theorie der brownschen molekularbewegung und der suspensionen. *Annalen der Physik*, 326(14):756–780, 1906.

[54] N. Yasuda and M. Kimura. A study of human migration in the mishima district. *Ann. Hum. Genet.*, 36:313–323, 1973.

[55] D. Young and R. Bettinger. Simulating the global human expansion in the late pleistocene. *J. Archaeol. Sci.*, 22:89–92, 1995.

7 Appendix A

So far we based all considerations on constant, not-changing environmental conditions which are expressed by constant model parameters (such as the growth coefficient a and the carrying capacity K). However, this assumption is not always realistic. In fact changes in environmental conditions are rather the norm than the exception. We can account for such changes by allowing the model parameter to be time-dependent.

The aim of this appendix is to illustrate the effects of different temporal change patterns of the model parameters a and K on the population's growth behaviour. Thereby we assume the following temporal change patterns

1. linear model: $a(t) = a_0(1 - ct)$,
2. exponential model: $a(t) = a_0 e^{ct}$ respectively $K(t) = K_0 e^{ct}$,
3. sinusoidal model: $a(t) = a_0 + a_m \sin \omega t$ respectively $K(t) = K_0 + K_m \sin \omega t$ where a_m and K_m describe the amplitudes, $\omega = \frac{2\pi}{T}$ the frequency and T the period of the sinus wave.

To understand the impacts of temporal varying $a(t)$ and $K(t)$ in detail we investigate the effects of changes in the model parameter separately. That means we assume that one coefficient is constant and the other is changing over time.

Logistic growth

We start with the bounded logistic growth process and generalise the logistic model (11) by allowing for variable growth rate $a(t)$ and carrying capacity $K(t)$

$$\frac{\partial u}{\partial t}(t) = a(t)\left(1 - \frac{u}{K(t)}(t)\right) u(t). \tag{21}$$

Figures 34-36 show the resulting growth behaviour of the population under the assumptions 1-3 for the growth coefficient a and contrary, Figures 37 and 38 illustrate the growth dynamic under varying carrying capacities according to assumptions 2 and 3.

Figure 34 shows the population's growth behaviour for a linearly varying growth coefficient $a(t) = a_0(1 + ct)$ with different slopes c. For $c = -0.5$ the growth parameter a decreases so strongly over time (in fact even becomes negative) that the population goes extinct. For $c = -0.1$ the growth parameter decreases, too, however the population size tends to a certain threshold $0 < u^\star < K$ which is smaller then the carrying capacity. The value $c = 0$ coincides with the situation of constant coefficients and for $c = 0.1; 0.5$ the growth parameter a are increasing what results in a faster convergence toward K.

A similar behaviour can be seen in Figure 35 where an exponential change pattern $a(t) = a_0 e^{ct}$ is assumed. Here the case $c = -0.5$ does not result in the population extinction (cf. red line in Figure 35).

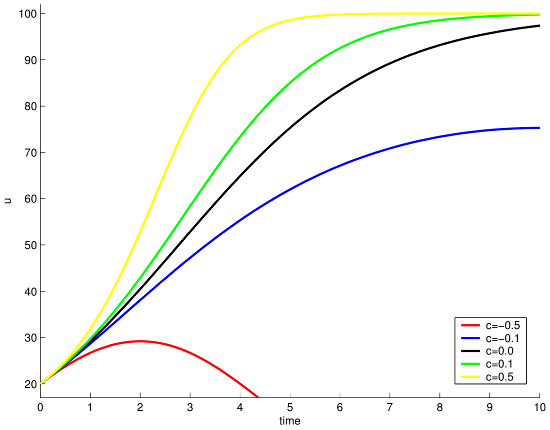

Figure 34: Population growth under the assumption of linear temporal changes of the growth coefficient: $a(t) = a_0(1 + ct)$ with $a_0 = 1$ and $c = -0.5; -0.1; 0; 0.1; 0.5$.

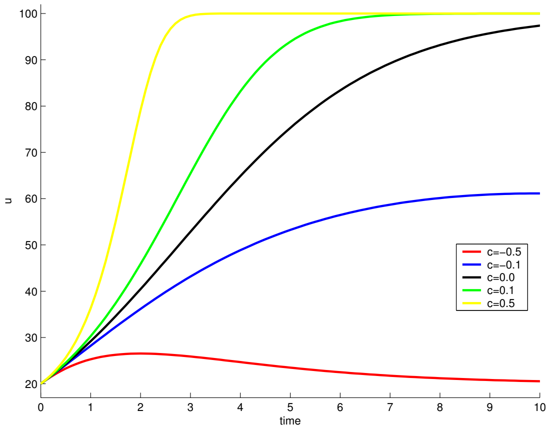

Figure 35: Population growth under the assumption of exponential temporal changes of the growth coefficient: $a(t) = a_0 e^{ct}$ with $a_0 = 1$ and $c = -0.5; -0.1; 0; 0.1; 0.5$.

Figure 36 shows the impact of a cyclic behaviour $a(t) = a_0 + a_m \sin \omega t$, $a_0 = 0.2, T = 5$ of the growths coefficient. The population size over time reflects these cycles and we observe a non-steady population growth.

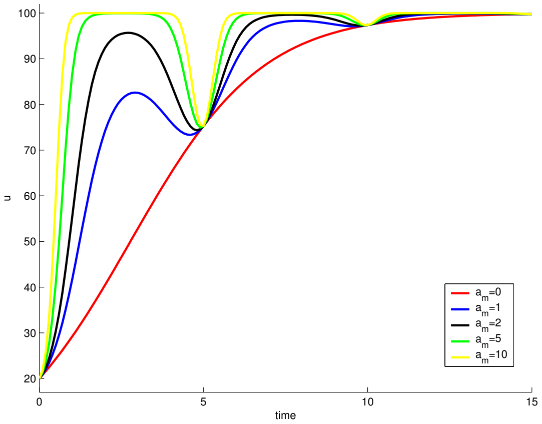

Figure 36: Population growth under the assumption of sinusoidal temporal changes of the growth coefficient: $a(t) = a_0 + a_m \sin \omega t$ with $a_0 = 0.2$, $T = 5$ and $a_m = 0; 1; 2; 5; 10$

Now we turn to analysing the impacts of temporal varying carrying capacities $K(t)$. Figure 37 shows exponential carrying capacities (dashed lines) $K(t) = K_0 e^{ct}$ for different parameters c and the resulting population's growth dynamic (solid lines). For $c = -0.5; -0.1$ the carrying capacity tends to zero, that means there is no possibility for populations to survive (cf. red and blue lines). Contrary, for increasing carrying capacities (cf. yellow and green lines) we see a sharp increase in population size. If the carrying capacity possesses a cyclic behavior of the form $K(t) = K_0 + K_m \sin \omega t$ then we also see a cyclic pattern in the population size (cp. figure 44). Interestingly, Figure 39 shows that the response of the population size to changes in the carrying capacity has a time delay.

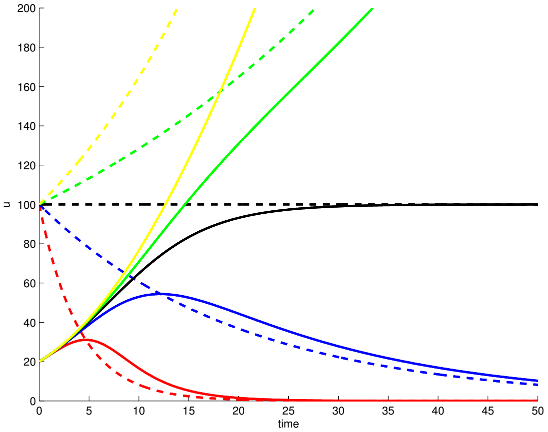

Figure 37: Population growth under the assumption of exponential temporal change $K(t) = K_0 e^{ct}$ with $K_0 = 100$ and $c = -0.5; -0.1; 0; 0.1; 0.5$

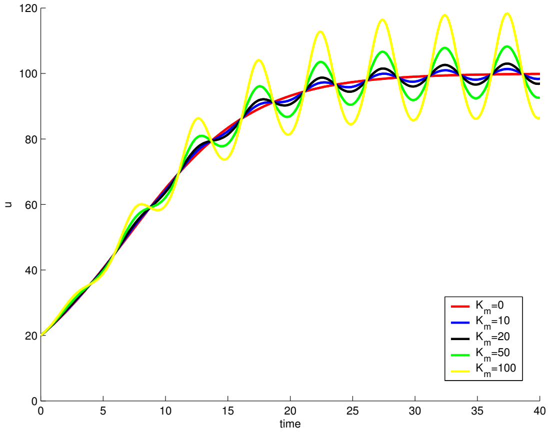

Figure 38: Population growth under the assumption of sinusoidal temporal change $K(t) = K_0 + K_m \sin \omega t$ with $K_0 = 100$, $K_m = 0; 10; 20; 50; 100$ and $T = 5$

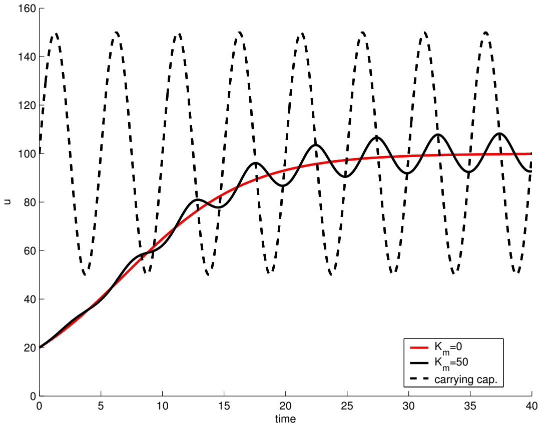

Figure 39: Population growth under the assumption of sinusoidal temporal change $K(t) = K_0 + K_m \sin \omega t$ (dashed line) with $K_0 = 100$, $K_m = 0; 50$ and $T = 5$ (solid lines)

Confined exponential growth

In this section we generalise model (13) by assuming different temporal change patterns for the growth coefficient a and the carrying capacity K.

Figure 40 illustrates the confined exponential growth assuming a linear temporal change of the growth coefficient $a(t) = a_0(1 + ct$ with different slopes c. The growth behaviours are similar to the logistic case (cp. Figure 34). For $c = -0.5; -0.1$ the growth coefficient $a(t)$ is decreasing with time (it even becomes negative) and consequently the population goes extinct (cf. red and blue lines). The value $c = 0$ coincides with the case of constant coefficients and for $c = 0.1; 0.5$ the growth coefficient increases over time which results in a fast convergence toward K.

A similar behavior can be seen in Figure 41 where the confined exponential growth with

$a(t) = a_0 e^{ct}$ is illustrated. However, for $c = -0.5; -0.1$ the populations size converges to a stable equilibrium $u^\star = K - (K - u_0)e^{\frac{a_0}{c}} < K$.

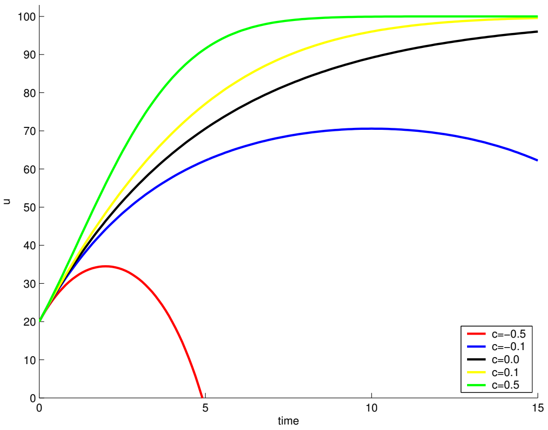

Figure 40: Population growth under the assumption of linear temporal changes of the growth coefficient: $a(t) = a_0(1 + ct)$ with $a_0 = 1$ and $c = -0.5; -0.1; 0; 0.1; 0.5$.

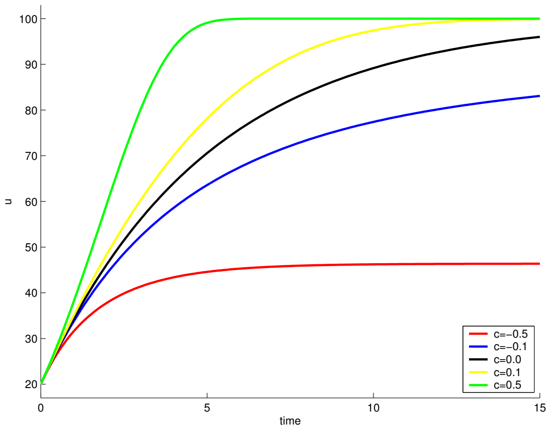

Figure 41: Population growth under the assumption of exponential temporal changes of the growth coefficient: $a(t) = a_0 e^{ct}$ with $a_0 = 1$ and $c = -0.5; -0.1; 0; 0.1; 0.5$.

Further, if we assume a cyclic temporal change pattern for the growth coefficient $a(t) = a_0 + a_m \sin \omega t$ we obtain a cyclic but generally increasing population size (cf. Figure 42).

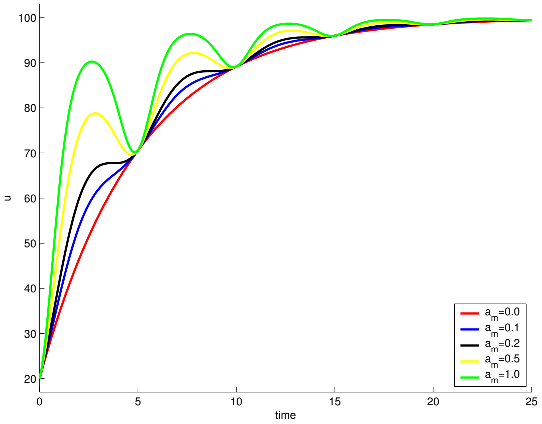

Figure 42: Population growth under the assumption of sinusoidal temporal changes of the growth coefficient: $a(t) = a_0 + a_m \sin \omega t$ with $a_0 = 0.2$, $T = 5$ and $a_m = 0; 0.1; 0.2; 0.5; 1$

Lastly we consider the effects of temporally changing carrying capacities on the growth dynamic. Figure 43 shows the exponential carrying capacities (dashed lines) $K(t) = K(t) = K_0 e^{ct}$ and the corresponding confined exponential growth (solid lines). For $c = -0.5; -0.1$ the carrying capacity tend to zero, and consequently the population goes extinct. If the carrying capacity possesses a cyclic behavior of the form $K(t) = K_0 + K_m \sin \omega t$ then this behavior is reflected in the growth behaviour of the population (cp. Figure 44).

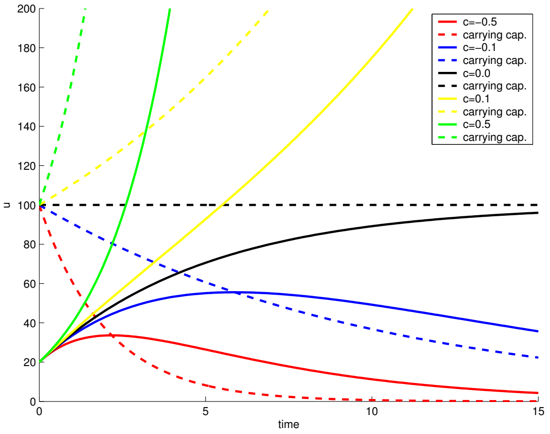

Figure 43: Population growth under the assumption of exponential temporal change $K(t) = K_0 e^{ct}$ with $K_0 = 100$ and $c = -0.5; -0.1; 0; 0.1; 0.5$

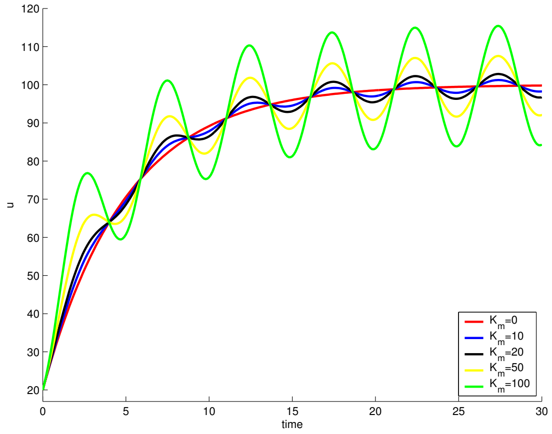

Figure 44: Population growth under the assumption of sinusoidal temporal change $K(t) = K_0 + K_m \sin \omega t$ with $K_0 = 100$ and $K_m = 0; 10; 20; 50; 100$

8 Appendix B

Not only temporal also spatial variation in the environmental conditions will impact the spread dynamic of a population. We would e.g. expect that populations spread/grow faster in lowlands compared to mountain regions or in hospitable habitats compared to inhospitable habitats. In order to account for environmental heterogeneities we need to allow for spatially variable model parameters $a = a(x)$, $D = D(x)$ and $K = K(x)$ which reflect those changing environmental conditions. Exemplarily the diffusion-reaction model with logistic growth is in this way generalised to

$$\frac{\partial u}{\partial t}(t,x) = D(x) \triangle u(t,x) + a(x)u(t,x)\left(1 - \frac{u(t,x)}{K(x)}\right).$$

Also the interaction dynamic between different populations will be influenced by spatial environmental heterogeneities significantly. One population may e.g. be well-adopted to a particular habitat whereas the other population is well-adapted to another, different, habitat. Consequently both populations have a competitive advantage in their preferred habitats.

To model those spatial differences we assume that the domain $\mathbb{D}$ is divided into two sub-domains $\mathbb{D}_1$ and $\mathbb{D}_2$ and it holds for the competition coefficients c_{12} and c_{21}

$$c_{12}(x) = \begin{cases} b_1 & \text{if } x \in \mathbb{D}_1 \\ b_2 & \text{if } x \in \mathbb{D}_2 \end{cases} \qquad \text{and} \qquad c_{21}(x) = \begin{cases} b_2 & \text{if } x \in \mathbb{D}_1 \\ b_1 & \text{if } x \in \mathbb{D}_2 \end{cases} \qquad \text{with } b_1 < b_2.$$

Summarising we can generalise our competition approach (19) by allowing the model parameter to be spatially dependent

$$\begin{aligned} \frac{\partial u_1}{\partial t} &= d_1(x)\triangle u_1 + a_1(x)u_1\left(1 - \frac{u_1}{K_1(x)} - c_1(x)\frac{u_2}{K_1(x)}\right) \\ \frac{\partial u_2}{\partial t} &= d_2(x)\triangle u_2 + a_2(x)u_2\left(1 - \frac{u_2}{K_2(x)} - c_2(x)\frac{u_1}{K_2(x)}\right). \end{aligned}$$

Due to the assumed dominance of each population in its core area ($\mathbb{D}_1$ and $\mathbb{D}_2$), each population is immune to extinction in its own core area. But the diffusion mechanism is able to produce a stable interaction or coexistence zone between the two core areas. Figure 45 shows the stable long-term frequencies of both populations for different values of the diffusion coefficients D_i, the measure of the tendency to spread in space. It is obvious that the equilibria are not spatially constant. The larger the diffusivity, i.e., the further the individuals of one population are able to spread into the core area of the other population, the wider is the stable coexistence zone (cf. Figure 45). Spatial spread can even mix both populations in such a way that they are both present over the whole considered area $\mathbb{D}$ (cf. Figure 45 (left)). Therefore, the inclusion of spatial heterogeneity to model (19) in the form of spatial varying competition behavior leads to more complex situations, where, due to the assumed dominance of both populations in their core areas, coexistence is possible. The width of the interaction zone depends on the tendency of individuals of both populations to be spatially mobile outside their own core areas.

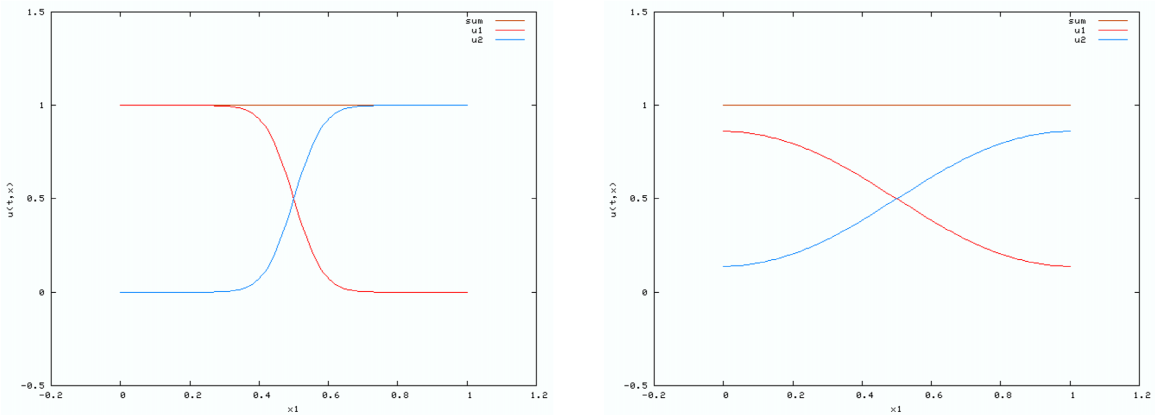

Figure 45: Stable long term frequencies of both populations under (left) low diffusivities and (left) high diffusivities.